Purine nucleosides interfere with c-di-AMP levels and act as adjuvants to re-sensitise MRSA to β-lactam antibiotics

Aaron C. Nolan[a^], Merve S. Zeden[a^#], Christopher Campbell[a], Igor Kviatkovski[b], Lucy Urwin[c], Rebecca M. Corrigan[c], Angelika Gründling[b], and James P. O'Gara[a#]

[a]Microbiology, School of Biological and Chemical Sciences, University of Galway, H91 TK33, Ireland.

[b]Section of Molecular Microbiology and Medical Research Council Centre for Molecular Bacteriology and Infection, Imperial College London, London, SW7 2AZ, United Kingdom.

[c]The Florey Institute, School of Bioscience, University of Sheffield, Sheffield, S10 2TN, United Kingdom.

^These authors contributed equally

[#]To whom correspondence should be addressed: merve.zeden@nuigalway.ie and jamesp.ogara@nuigalway.ie

Article word count (Introduction, Results & Discussion): 5,435

Keywords: *Staphylococcus aureus*, MRSA, purine metabolism, antibiotic adjuvant, β-lactam resistance, c-di-AMP.

Running title: Purine nucleosides resensitise MRSA to β-lactam antibiotics

Abstract

Elucidating the complex mechanisms controlling *mecA*/PBP2a-mediated β-lactam resistance in methicillin resistant *Staphylococcus aureus* (MRSA) has the potential to identify new drug targets with therapeutic potential. Here, we report that mutations that interfere with *de novo* purine synthesis (*pur* operon), purine transport (NupG, PbuG and PbuX) and the nucleotide salvage pathway (DeoD2, Hpt) increased β-lactam resistance in MRSA strain JE2. Extrapolating from these findings, exogenous guanosine and xanthosine, which are fluxed through the GTP branch of purine biosynthesis were shown to significantly reduce MRSA β-lactam resistance. In contrast adenosine, which is fluxed to ATP, significantly increased oxacillin resistance, whereas inosine, which can be fluxed to ATP and GTP via hypoxanthine, only marginally reduced the oxacillin MIC. Increased oxacillin resistance of the *nupG* mutant was not significantly reversed by guanosine, indicating that NupG is required for guanosine transport, which in turn is required to reduce β-lactam resistance. Suppressor mutants resistant to oxacillin/guanosine combinations contained several purine salvage pathway mutations, including *nupG* and *hpt*. Microscopic analysis revealed that guanosine significantly increased cell size, a phenotype also associated with reduced levels of c-di-AMP. Consistent with this, guanosine significantly reduced levels of c-di-AMP, and inactivation of GdpP, the c-di-AMP phosphodiesterase negated the impact of guanosine on β-lactam susceptibility. PBP2a expression was unaffected in *nupG* or *deoD2* mutants suggesting that guanosine-induced β-lactam susceptibility may result from dysfunctional c-di-AMP-dependent osmoregulation. These data reveal the therapeutic potential of purine nucleosides as β-lactam adjuvants that interfere with the normal activation of c-di-AMP required for high-level β-lactam resistance in MRSA. 249 words

Importance

The clinical burden of infections caused by antimicrobial resistant (AMR) pathogens is a leading threat to public health. Maintaining the effectiveness of existing antimicrobial drugs or finding ways to reintroduce drugs to which resistance is widespread is an important part of efforts to address the AMR crisis. Predominantly the safest and most effective class of antibiotics are the β-lactams, which are no longer effective against

methicillin resistant *Staphylococcus aureus* (MRSA). Here we report that the purine nucleosides guanosine and xanthosine have potent activity as adjuvants that can resensitise MRSA to oxacillin and other β-lactam antibiotics. Mechanistically, exposure of MRSA to these nucleosides significantly reduced the levels of the cyclic dinucleotide c-di-AMP, which is required for β-lactam resistance. Drugs derived from nucleotides are widely used in the treatment of cancer and viral infections highlighting the clinical potential of using purine nucleosides to restore or enhance the therapeutic effectiveness of β-lactams against MRSA and potentially other AMR pathogens. 156 words

Introduction

Staphylococcus aureus is an opportunistic pathogen responsible for localised skin infections and more severe illnesses, such as bacteraemia, sepsis, infectious arthritis, pneumonia, endocarditis, urinary tract infections and toxic shock syndrome (1, 2). While significant advances have been made in our understandings of the metabolism of *S. aureus* in recent years, we have only just begun to interrogate the role of central metabolic pathways required for bacterial proliferation in the host, and their contribution to antibiotic resistance.

β-lactam antibiotics remain a gold standard for the treatment of *S. aureus* infections, while vancomycin and daptomycin are recommended for methicillin resistant *S. aureus* (MRSA) infections (3-6). However, while effective, these antibiotics are limited by slow bactericidal activity, low tissue penetration, and nephrotoxicity (7, 8). Daptomycin exhibits high protein binding and low serum concentrations which necessitates high doses of the antibiotic to achieve therapeutic levels (9). Limited treatment options for MRSA infections are exacerbated by the emergence of vancomycin intermediate *S. aureus* (VISA) strains that also display a 100-fold decrease in susceptibility to daptomycin (10, 11).

MRSA resistance to β-lactam antibiotics such as methicillin that are not cleaved by bacterial β-lactamases, is mediated through the expression of the low affinity penicillin binding protein PBP2a, encoded by the *mecA* gene located on the mobile genetic element, the staphylococcal chromosome cassette (SCC*mec*) (12, 13). The PBP2a

88 transpeptidase crosslinks peptidoglycan in the presence of β-lactam antibiotics to
89 confer resistance (13-15).
90 Carriage of SCC*mec* is linked to heterogenous, low-level resistance (HeR) to β-lactam
91 antibiotics (13, 16). Deregulation of *mecA* transcription occurs when the MecR sensor-
92 protease is activated by the presence of β-lactams resulting in cleavage of the MecI
93 repressor (17). When exposed to β-lactam antibiotics, high-level, homogeneously
94 resistant (HoR) MRSA mutants carrying accessory mutations outside SCC*mec* can
95 also be selected (18, 19). Commonly, these mutations lead to activation of the
96 stringent response (20, 21), increased cyclic di-adenosine monophosphate (c-di-AMP)
97 levels (22-24), changes in the activity of RNA polymerase (6), as well as the ClpXP
98 chaperone-protease complex (25, 26).
99 Nucleotide second messengers play an important role in the control of β-lactam
100 resistance. Nucleotides are essential precursors used by all cells for DNA, RNA and
101 signalling molecule synthesis, while the energy carriers, adenosine-triphosphate
102 (ATP) and guanosine-triphosphate (GTP), are produced from their corresponding
103 nucleotides adenine and guanine (27, 28). Bacteria utilise an array of nucleotide
104 secondary messengers to regulate cellular responses to fluctuations in external stimuli
105 and environmental conditions (29). Bacterial nucleotide messengers are typically
106 produced from the building blocks ATP and GTP (30). Refined signal transduction
107 pathways are necessary for *S. aureus* to survive and multiply during infection. Signal
108 transduction in *S. aureus* influences virulence gene expression during infection, stress
109 and antibiotic survival responses (31, 32).
110 *S. aureus* produces ATP/GTP through a *de novo* ten-step biosynthetic process. The
111 *pur* operon encodes ten enzymes that first convert ribose-5-phosphate (Ribose-5-P)
112 to inosine monophosphate (IMP); the branchpoint between ATP and GTP synthesis
113 (Fig. 1). IMP can then be converted to adenosine monophosphate (AMP) or
114 xanthosine monophosphate (XMP) through *purA/purB* or *guaA* respectively. AMP is
115 then converted to adenosine diphosphate (ADP), ATP and c-di-AMP. On the alternate
116 branch XMP is converted to guanosine diphosphate (GDP), GTP and guanosine
117 tetraphosphate/pentaphosphate (ppGpp/(p)ppGpp) which promotes accumulation of
118 c-di-AMP by repressing the activity of the c-di-AMP phosphodiesterase GdpP (33).
119 Alternatively, XMP, GMP and AMP can be produced from nucleosides/nucleotides

120 through the purine salvage pathway, including transport by the purine transporters
121 PbuX, PbuG and NupG. There is ongoing interest in purine metabolism due to its
122 multifaceted roles in biofilm formation, virulence and antibiotic resistance (34-36).
123 The alarmones ppGpp and pppGpp play a central role in the stringent response, while
124 c-di-AMP contributes to the regulation of cell envelope homeostasis, osmotic
125 regulation and virulence (37-40). Altering c-di-AMP levels and/or (p)ppGpp levels lead
126 to differences in β-lactam susceptibility of MRSA strains (31, 41). Mutation of the
127 diadenylate cyclase gene *dacA*, leading to reduced c-di-AMP levels, resulted in the
128 conversion of an HoR MRSA to a HeR strain (31). Conversely inactivating mutations
129 in the c-di-AMP phosphodiesterase gene *gdpP* leading to increased c-di-AMP levels
130 were accompanied by homogeneous resistance to methicillin (22, 23). GdpP activity
131 is repressed by ppGpp, which is synthesised by the RelI, RelP and RelQ enzymes (41-
132 43). In several studies it has been reported that activation of the stringent response
133 and constitutive (p)ppGpp production, which will increase c-di-AMP levels (33), are
134 accompanied by homogeneous methicillin resistance (21, 44). The importance of
135 these signalling molecules to bacterial survival under different growth conditions and
136 their absence in humans marks them as attractive antimicrobial drug targets (45).
137 Further understanding of molecular mechanisms to antibiotic resistance is an
138 important part of efforts to identify new targets with the potential to re-sensitise bacteria
139 to antibiotics including β-lactams (46). The knowledge gained from understanding
140 such molecular mechanisms could be used to identify compounds that provide
141 synergistic activity with β-lactams, thus providing a potential solution to antibiotic
142 resistance and dwindling antibiotic therapy options (47-49).
143 In this study, the impact of exogenous purines on growth and susceptibility to β-
144 lactams and other antibiotics is described in several strains of *S. aureus* and MRSA,
145 and *S. epidermidis*. The contribution of several genes involved in *de novo* purine
146 synthesis, purine transport, purine salvage, and (p)ppGpp/c-di-AMP signalling to
147 nucleoside/β-lactam susceptibility has been elucidated. Our data reveal that re-
148 sensitisation of MRSA to β-lactams using guanosine or xanthosine is dependent on
149 several purine transporters and salvage pathway enzymes, and accompanied by
150 increased cell size and reduced levels of c-di-AMP. The therapeutic potential of using
151 purine nucleosides as β-lactam antibiotic adjuvants is discussed.

152 **Results**

153

154 **Exogenous purines regulate MRSA growth and susceptibility to β-lactam**
155 **antibiotics.** The correlation between increased levels of the purine signalling
156 nucleotides (p)ppGpp and c-di-AMP and increased resistance to β-lactam antibiotics
157 raises the possibility that manipulation of purine metabolism (Fig. 1) by controlling the
158 availability of purines in the growth environment can regulate the susceptibility of
159 MRSA to β-lactam antibiotics. Exogenous purines transported into the cell are
160 metabolised via the purine salvage pathway (Fig. 1). Growth of wild-type MRSA strain
161 JE2 at oxacillin (OX) concentrations of 1, 16, 32 or 64 μg/ml was measured in
162 chemically defined media without glucose (CDM) supplemented with both adenine and
163 guanine, without adenine and guanine, with adenine alone or with guanine alone.
164 Weak growth at the lowest OX concentration in CDM with both adenine and guanine
165 was only measured after >30 h (Fig. S1A). This was significantly improved in CDM
166 lacking both guanine and adenine (Fig. S1B) and growth in OX 1 μg/ml was also
167 measured in CDM with adenine alone (Fig. S1C). Strikingly, JE2 was completely
168 susceptible to OX in CDM supplemented with guanine alone, with no growth detected
169 even after 48 h (Fig. S1D).
170 Switching to nucleosides, which are more readily solubilised in water than nucleotides,
171 and Mueller Hinton 2% NaCl broth (MHB), which is routinely used for antibiotic
172 susceptibility testing, addition of guanosine or xanthosine rendered JE2 susceptible to
173 OX with the minimum inhibitory concentration (MIC) reduced from 64 to ⩽4 μg/ml
174 (Table 1). In contrast, JE2 was significantly more resistant to OX in MHB
175 supplemented with adenosine (MIC = 256 μg/ml, Table 1). Interestingly,
176 supplementation of MHB with up to 1.0 g/l inosine, which can be fluxed to both the
177 ATP and GTP branches of purine biosynthesis via hypoxanthine and IMP (Fig. 1) only
178 marginally reduced the JE2 OX MIC to 32 μg/ml. Similarly, OX susceptibility was
179 unchanged in MHB supplemented with both guanosine and adenosine (MIC = 64
180 μg/ml). Disk diffusion assays on MHA showed that exogenous guanosine also
181 increased the susceptibility of JE2 to other β-lactam antibiotics, namely cefotaxime,
182 cefoxitin, cefaclor and penicillin G (Fig. 2A, B), but did not show any synergy with
183 tetracycline, vancomycin, chloramphenicol, and gentamicin (Fig. 2C).

184 Checkerboard titration assays further revealed that guanosine increased JE2
185 susceptibility to OX in a concentration-dependent manner (Fig. S2). In time kill assays,
186 combinations of guanosine and OX achieved a significant ≥2 $\log^{10}$ reduction in the
187 number of colony forming units (CFU)/ml over 12 hours compared to OX alone, and
188 achieved bactericidal activity at OX concentrations > 64 μg/ml (Fig. S3). At lower OX
189 concentrations, recovery of JE2 growth after 12 hours, presumably reflected the
190 selection and expansion of suppressors or OX HoR mutants as described previously
191 (22, 50, 51).
192 This evident synergy between OX and the purine nucleosides guanosine and
193 xanthosine versus the antagonism with adenosine and the relatively neutral effect of
194 inosine implicate purine nucleotide homeostasis in the control of MRSA β-lactam
195 susceptibility.
196
197 **Purine nucleoside-regulated β-lactam resistance in other *S. aureus* strains and**
198 ***S. epidermidis* RP62A.** Extending these analyses to other staphylococcal strains
199 revealed that guanosine and xanthosine also reduced the OX MICs of several
200 heterogeneously resistant MRSA strains to varying levels; USA300 (SCC*mec* type IV,
201 CC8), MW2 (SCC*mec* type IV; CC1), DAR13 (SCC*mec* type IV; CC8), DAR173
202 (SCC*mec* type IV; CC5), DAR169 (SCCmec type I; CC8), DAR45 (SCC*mec* type II;
203 CC30), DAR22 (SCC*mec* type III; CC5) and methicillin resistant *S. epidermidis* RP62A
204 (Table 1, Table S1). Guanosine at 1 g/l was only associated with a 1-fold reduction in
205 the OX MICs of the homogeneously resistant MRSA strains COL (SCC*mec* I, CC8)
206 and BH1CC (SCC*mec* II, CC8) (Table 1), suggesting that genetic changes associated
207 with high-level methicillin resistance can potentially negate the ability of purine
208 nucleosides to reduce β-lactam resistance of MRSA. Interestingly guanosine and
209 xanthosine also significantly reduced the OX MIC for the methicillin susceptible
210 laboratory strain 8325-4 and the Nebraska transposon library (NTML) (52) *mecA*
211 mutant NE1868, while adenosine increased their OX MICs indicating that therapeutic
212 potential of purine nucleosides to control MRSA and MRSE β-lactam susceptibility is
213 both *mecA*-dependent and *mecA*-independent.
214
215 **Mutations in the *de novo* purine biosynthesis or purine salvage pathways**
216 **increase resistance to β-lactam antibiotics.** Next the impacts of mutations in the *de*

217 *novo* purine synthesis *pur* operon and purine salvage pathways (Fig. 1) on β-lactam
218 resistance were investigated. NTML mutations in all tested *pur* operon genes (except
219 *purH*) increased OX resistance, whereas mutation of the *purR* repressor gene was
220 accompanied by increased OX susceptibility (Table 1). OX resistance was also
221 increased in mutants of the putative transporters *nupG* (NE1419, guanine/guanosine),
222 *pbuG/stgP* (NE283, guanine/hypoxanthine), *pbuX* (NE280, xanthine/xanthosine) and
223 a predicted purine nucleoside phosphorylase *deoD2* (NE650) (Table 1). Consistent
224 with the predicted roles of these nucleoside transporters, xanthosine reduced the
225 oxacillin MIC of the *nupG* mutant and guanosine reduced OX resistance of the *pbuX*
226 mutant (Table 1). These data suggest that NupG is the major guanosine transporter
227 and PbuX is the main xanthosine transporter under the conditions tested. Both
228 guanosine and xanthosine reduced OX resistance of the *pbuG* mutant (Table 1), which
229 was previously shown to transport guanine (53). The very subtle effect of inosine on
230 the OX MIC precluded investigation of the possible roles of NupG, PbuG and PbuX in
231 inosine transport using susceptibility testing. Interestingly xanthosine, but not
232 guanosine, significantly reduced the OX MIC of the *deoD2* mutant (Table 1), indicating
233 that xanthosine can be phosphorylated by a different enzyme during purine salvage.
234 The most likely candidate is a second putative nucleoside phosphorylase DeoD1
235 (NE477), which shares 67.4% identity with DeoD2 (Fig. S4A). Mutation of *deoD1* alone
236 did not impact oxacillin susceptibility and both guanosine and xanthosine reduced the
237 OX MIC of this mutant (Table 1), suggesting that DeoD1 and DeoD2 may be able to
238 substitute for each other in the phosphorylation of xanthosine under specific growth
239 conditions. Finally, in keeping with the prediction that guanine and xanthine are
240 processed by different phosphoribosyltransferase enzymes (Hpt and Xpt, respectively,
241 Fig. 1), xanthosine but not guanosine also reduced the OX MIC by 4-5 fold in the *hpt*
242 mutants R10 and R11 carrying $S_{71}C$ and $T_{61}P$ substitutions, respectively (53) (Table
243 1).
244 To verify that the *nupG* and *deoD2* mutations were responsible for increased OX
245 resistance in NE1419 and NE650, the *nupG*::Erm^r and *deoD2*::Erm^r alleles were
246 transduced using phage 80α into wild-type JE2 and MW2 (Table S1). The OX MICs
247 of the resulting transductants were the same as NE1419 and NE650, i.e. 128 μg/ml.
248 The NE1419 and NE650 mutants were also complemented by the respective wild-type

249 genes cloned into pLI50 (Fig. S4B and C, Table 1), restoring OX sensitivity and
250 confirming the specific role of each in the resistance phenotype. Using Western blot
251 analysis, no differences were detected in PBP2a expression levels in these mutants
252 and their complemented derivatives compared to wild-type JE2 (Fig. S4D).
253 Collectively these data are consistent with the role of purine biosynthesis and salvage
254 in the regulation of MRSA β-lactam resistance, via a mechanism that is independent
255 of PBP2a.
256
257 **Exogenous nucleosides control MRSA growth, cell size and β-lactam**
258 **susceptibility in a NupG-dependent manner.** Given their role as potential carbon
259 sources, the impact of exogenous nucleosides on the growth of MRSA, which may in
260 turn influence antibiotic resistance, was investigated. Weak JE2 growth in OX 1, 16 or
261 32 μg/ml (Fig. 3A) was completely inhibited by 0.2 g/l guanosine (Fig. 3B). In contrast,
262 the increased OX resistance of the *nupG* mutant was not significantly reversed by
263 guanosine (Fig. 3A, B), indicating again that NupG is the main guanosine transporter
264 in *S. aureus* under the growth conditions tested. JE2 growth in OX was also inhibited
265 by 0.2 g/l xanthosine (Fig. 3C), but was unaffected in MHB 0.2 g/l adenosine (Fig. 3D).
266 Consistent with the likely role of PbuX in xanthosine transport, growth of the *nupG*
267 mutant in OX was significantly inhibited by xanthosine (Fig. 3C), and like the wild-type
268 was largely unaffected by adenosine (Fig. 3D).
269 Strikingly, guanosine significantly increased the optical density (OD_{600}) of JE2
270 cultures, whereas adenosine negatively impacted growth and xanthosine had no effect
271 (Fig. 4A). However, enumeration of JE2 colony forming units (CFUs) revealed no
272 significant differences between MHB or MHB supplemented with guanosine,
273 xanthosine or adenosine (Fig. 4B). For the *nupG* mutant, exogenous guanosine or
274 xanthosine did not significantly affect growth, but cell density (OD_{600}) was significantly
275 reduced by adenosine (Fig. 4C). CFU numbers for *nupG* cultures were unaffected by
276 any nucleoside (Fig. 4D). Given that all three of these ribose-containing nucleosides
277 have the potential to serve as carbon sources, their different effects on cell density
278 indicates that their impact on β-lactam susceptibility was not a nutritional effect.
279 A recent study revealed that exposure to OX increases *S. aureus* cell size and leads
280 to cell division defects (54). To investigate the impact of exogenous guanosine on

281 morphology and cell size, which can impact growth culture optical density, confocal
282 microscopy experiments were performed on cells collected from JE2 cultures grown
283 in MHB NaCl, MHB NaCl OX, MHB NaCl Gua and MHB NaCl OX/Gua and stained
284 with Vancomycin-BODIPY or WGA Alexa Fluor 594 (Fig. 5A, B). The diameter of cells
285 grown in guanosine was slightly, yet significantly, increased compared to cells grown
286 in MHB NaCl only. Cell size was further increased in cells grown in oxacillin, with the
287 largest cell size measured in the OX/Gua combination (Fig. 5A, B). Increased cell size
288 may explain, at least in part, why exogenous guanosine increased the optical density
289 (OD_{600}) of JE2 cultures, independent of changes in the number of CFUs. Furthermore,
290 the dramatic effect of the OX/Gua combination on both increased β-lactam
291 susceptibility and cell size raised the possibility that these phenotypes are associated
292 with altered regulation of c-di-AMP, which as noted earlier is known to control both of
293 these phenotypes (37-40).
294
295 **Suppressor mutations in purine metabolism, transcriptional and translational**
296 **regulation and ClpX overcome MRSA susceptibility to oxacillin/purine**
297 **combinations.** Repetitive passaging experiments in MHB 2% NaCl supplemented
298 with OX (32 μg/ml) and guanosine (0.2 g/l) were used to isolate suppressor mutants
299 resistant to the OX/Gua combination. For control purposes, HoR mutants isolated from
300 JE2 grown in medium supplemented with OX alone (32 μg/ml) were also isolated. In
301 total 16 OX/Gua suppressor mutants and 4 HoR mutants that exhibited stable
302 resistance to oxacillin were characterised and sequenced (Table 2). All 16 OX/Gua
303 suppressor mutants exhibited higher MICs to OX, OX/Gua and OX/Xan combinations
304 (Table 2). Several mutations directly impacted purine biosynthetic and salvage
305 pathways supporting the hypothesis that purine homeostasis controls β-lactam
306 resistance. The identification of a W_{29}Stop suppressor mutation in *nupG* (GS28) is
307 consistent with the phenotype of the *nupG* transposon mutant (NE1419) described
308 above. A *hpt* L_{113}Stop mutation was identified in suppressors GS8 and GS25 (Table
309 2) (Fig. 1). Consistent with the increased β-lactam resistance of GS8 and GS25, the
310 R10 and R11 *hpt* mutants (53) were also found to have an increased oxacillin MIC =
311 256 μg/ml (Table 1). However, in contrast the R10 and R11 *hpt* mutants (53) (Table
312 1), the oxacillin MIC of the GS8 and GS25 *hpt* null mutants was not substantially

313 reduced by xanthosine (Table 2), presumably due to the loss of Hpt activity in G8 and
314 GS25 versus altered Hpt activity of R10 and R11. Suppressor mutants GS15, GS16,
315 GS22 and GS23 carry $G_{35}D$ mutations in ribose-phosphate pyrophosphokinase (Prs),
316 which is responsible for the synthesis of phosphoribosyl diphosphate (PRPP), the
317 substrate for the *pur* operon-encoded enzymes. Mutations that may phenocopy
318 increased activity of the stringent response required for expression of high level β-
319 lactam resistance include RpoB mutations ($T_{480}K$ in GS4, GS29 and $T_{622}I$ in GS10,
320 GS17 and GS28) that lead to increased β-lactam resistance, increased doubling times
321 and thickened cell walls similar to increased Rel activity (44, 55-57), as well as
322 mutations that potentially impact translation (tRNA-Met in GS3, GS6, GS21, tRNA-Leu
323 in GS10 and tRNA-Ala in GS21, GS27). GS27 has a G_{278}Stop substitution in ClpX,
324 which is known to control β-lactam resistance (25). GS28 has a $A_{344}T$ substitution in
325 FemA previously implicated in resistance (58), as well as additional mutations in *rpoB*
326 and *nupG*. Similarly, the PdhB $G_{65}V$ mutations in GS16 and GS23 occur in conjunction
327 with Prs $G_{35}D$ substitutions and may further enhance growth and resistance in media
328 supplemented with OX/Gua. Mutations in *pdhB* were previously shown to confer a
329 growth advantage under osmotic stress (59).
330 The 4 Ox HoRs isolated for control purposes displayed varying MICs for OX/Gua and
331 OX/Xan, although all were more resistant to the combinations than the wild-type JE2
332 strain (Table 2). OS14, which has ClpX G_{98}Stop mutation was highly resistant to the
333 OX/Gua combination (MIC = 256 μg/ml), and even more resistant to the OX/Xan
334 combination (MIC = 256 μg/ml) than the GS1 and GS27 suppressor mutants with ClpX
335 G_{278}Stop mutations (MIC = 128 μg/ml). OS18 and OS30 were found to have $P_{101}H$
336 substitutions in RsbW, the anti-sigma factor that controls the activity of the alternative
337 sigma factor SigB, indicating that, consistent with a previous report (60), an altered
338 σ^B-mediated stress response can increase β-lactam resistance and partially overcome
339 susceptibility to the OX/Gua and OX/Xan combinations. Finally, a PBP2 $F_{44}S$
340 substitution in OS26 was associated with a modest increase in resistance to oxacillin,
341 and the OX/Gua and OX/Xan combinations (Table 2). Overall these data reveal that
342 aside from suppressors in the purine salvage pathway, mutations associated with the
343 HoR phenotype can also confer resistance to OX/nucleoside combinations.
344

345 **Guanosine-oxacillin combination treatment is associated with a *nupG* and**
346 ***deoD2*-dependent reduction in c-di-AMP levels.** The ATP and GTP-derived
347 stringent response alarmone (p)ppGpp and nucleotide second messenger c-di-AMP
348 regulate β-lactam resistance in MRSA (23, 31). Comparison of GTP levels using a
349 GTPase-Glo bioluminescence assay surprisingly revealed no significant differences
350 between JE2, *nupG* and *deoD2* grown in MHB NaCl supplemented with guanosine
351 (0.2 g/l) and/or oxacillin (1 or 32 μg/ml) (Fig. S5A). Using the same strains and growth
352 conditions, radiochemical thin layer chromatography (TLC) assays also to our surprise
353 revealed no significant differences in (p)ppGpp levels, except in JE2 grown in MHB
354 NaCl supplemented with guanosine (Fig. S5B). The absence of significant changes in
355 the stringent response alarmone in the *nupG* or *deoD2* mutants or during growth in
356 OX/Gua combinations revealed that guanosine/xanthosine-mediated increase in
357 oxacillin susceptibility is independent of (p)ppGpp signalling. Furthermore, the oxacillin
358 MIC of a rsh_{syn} mutant lacking three conserved amino acids in the (p)ppGpp synthetase
359 domain of the RSH (Rel) enzyme (33) was decreased and increased by
360 guanosine/xanthosine and adenosine, respectively, similar to the wild-type (Table 1)
361 further suggesting that these phenotypes are (p)ppGpp-independent.
362 A competitive ELISA assay revealed significantly reduced c-di-AMP levels in the *nupG*
363 and *deoD2* mutants grown in MHB NaCl (Fig. 6A) without oxacillin supplementation,
364 which may be in keeping with the disruption to the purine salvage pathway cause by
365 these mutations. Consistent with the putative role of NupG as a guanosine permease,
366 exogenous guanosine (0.2 g/l) did not impact c-di-AMP production in the *nupG* mutant
367 (Fig. 6A). Interestingly exogenous guanosine did restore c-di-AMP to wild-type levels
368 in the *deoD2* mutant (Fig. 6A), suggesting that even though this was not associated
369 with any change in oxacillin susceptibility (Table 1), the combination of NaCl and
370 imported guanosine leads to increased c-di-AMP production. This experiment was
371 repeated using MHB media without 2% NaCl (Fig. S6), which also showed that c-di-
372 AMP was reduced in the *nupG* and *deoD2* mutants, and that exogenous guanosine
373 restored c-di-AMP to wild-type levels in both mutants. Collectively, these data reveal
374 that *nupG* and *deoD2* mutations have robust impact on c-di-AMP in MHB and in MHB
375 NaCl. However, the data suggest that in the absence of NaCl, and oxacillin, alternative
376 permeases and nucleoside phosphorylases may substitute for the absence of NupG

377 and DeoD2 respectively, and restore c-di-AMP regulation and homeostasis.
378 Furthermore, NupG is a predicted sodium-nucleoside symporter, suggesting that in
379 the absence of sodium it will not import its substrate nucleoside.
380 Next, the levels of c-di-AMP were measured in the wild-type, *nupG* and *deoD2* strains
381 grown in MHB NaCl with OX, which are the same culture conditions used to measure
382 OX susceptibility. Given the negative effect of OX/Gua combinations on growth, the
383 culture volumes were scaled up for these experiments from 5 ml in 20 ml tubes (Fig.
384 6A) to 12 ml in 125 ml flasks (Fig. 6B). In contrast to growth in tubes (Fig. 6A), growth
385 in larger cultures volumes and flasks did not reveal any increase in wild-type c-di-AMP
386 levels in MHB NaCl supplemented with guanosine without OX (Fig. 6B), further
387 showing that changes in growth conditions can lead to differentially regulated c-di-
388 AMP levels in the cells. Importantly, the guanosine-induced OX susceptibility
389 phenotype of the wild-type correlated with the lowest levels of c-di-AMP compared to
390 growth in guanosine or OX alone (Fig. 6B). This significant effect was evident even
391 when very low, sub-MIC concentration (0.2 μg/ml) of OX used to minimise the effect
392 on growth. In contrast, growth of the *nupG* and *deoD2* mutants in MHB supplemented
393 with guanosine and OX increased c-di-AMP levels, albeit not reaching statistical
394 significance (Fig. 6C). The reduced levels of c-di-AMP in MRSA cells exposed to the
395 OX/Gua combination observed in this experiment is consistent with the significant
396 increase in cell size observed the same growth conditions (Fig. 5).
397 Consistent with an important role for c-di-AMP in these phenotypes, the increased OX
398 resistance of a Δ*gdpP*::Km mutant (ANG 1961) in which c-di-AMP levels are increased
399 (23) was unaffected by guanosine, xanthosine or adenosine even at 1 g/l (Table 1).
400 Similarly, the low OX MIC of a *dacA* $G_{206}S$ mutant in which c-di-AMP synthesis is
401 impaired but not abolished (61) was reduced further by exogenous guanosine or
402 xanthosine, and increased significantly by adenosine (Table 1). Overall these data
403 indicate that exogenous guanosine interferes with the normal activation of c-di-AMP
404 production required for full expression of β-lactam resistance in MRSA.
405

406 **Discussion**

407 Identification and characterisation of antibiotic adjuvants to maintain the therapeutic
408 effectiveness of currently licenced antibiotics, or facilitate the reintroduction of drugs
409 for which resistance is widespread, is a promising part of efforts to address the AMR
410 crisis. In keeping with previous studies implicating purine metabolism in the regulation
411 of MRSA β-lactam resistance (44, 62), we report here that mutations interfering with
412 the purine salvage and biosynthetic pathways increased oxacillin resistance. These
413 data prompted us to evaluate if the opposite was true and if susceptibility to β-lactams
414 could be increased by exposing MRSA to exogenous purine nucleotides and
415 nucleosides. Guanosine and xanthosine, which are fluxed through the GTP branch of
416 purine biosynthesis reduced the oxacillin MIC of JE2 into the susceptibility range, in a
417 dose dependent manner, whereas adenosine, which is fluxed to ATP, significantly
418 increased oxacillin resistance. Furthermore inosine, which can be fluxed to ATP or
419 GTP had almost no effect. These data reveal an important role for purine homeostasis
420 in controlling the susceptibility of MRSA to β-lactam antibiotics and add to several
421 recent studies implicating the regulation of purine biosynthesis in the control of
422 virulence (35, 63, 64). Interestingly, as part of a 2017 study from our laboratory
423 showing that β-lactams can attenuate MRSA virulence, transcriptomic analysis
424 revealed that, after the *agr* locus, the *pur* operon was the second most down-regulated
425 gene cluster during growth in oxacillin (50). Furthermore oxacillin-induced repression
426 of the *pur* operon was accompanied by significantly increased expression of *purR* (50),
427 a finding in keeping with the subsequent reports that PurR also acts as a repressor of
428 virulence (63, 64). Taken together, it appears that under β-lactam stress, MRSA may
429 attempt to limit flux through purine biosynthetic pathways as a means of increasing
430 resistance and that, conversely, increased guanosine or xanthosine flux into the GTP
431 branch of purine metabolism has the reverse effect and reduces β-lactam resistance.
432 A recent paper describing the interplay between *de novo* purine biosynthesis and c-
433 di-AMP signalling demonstrated that a *purF* mutation was associated with reduced
434 levels of c-di-AMP (35). Here we report that, with the exception of *purH*, mutations in
435 all other *pur* operon genes including *purF* were accompanied by increased β-lactam
436 resistance. The reduction in c-di-AMP levels in a *purF* mutant reported by Li et al (35)
437 and the increase in oxacillin resistance described in this study may at first appear to

438 be contradictory. However, it is important to note that the contribution of purine
439 homeostasis to β-lactam resistance can only be accurately characterised when MRSA
440 is grown in the presence of these antibiotics. Thus under standard growth conditions
441 (MHB NaCl media), our data showed that the purine salvage pathway *nupG* and
442 *deoD2* mutations were associated with reduced levels of c-di-AMP, whereas under
443 very mild oxacillin stress, c-di-AMP was restored to wild-type levels in these mutants.
444 Furthermore the reduced levels of c-di-AMP in wild-type exposed to the
445 guanosine/oxacillin combination was reversed in the *nupG* and *deoD2* mutants.
446 Among the purine metabolism mutations examined, *purH* and *deoD1* were not found
447 to have any impact on β-lactam resistance, although both mutants remained
448 susceptible to OX/Gua treatment. Purine nucleoside phosphorylases typically form
449 oligomers raising the possibility that DeoD1 and DeoD2 can heterodimerise, which
450 may influence their contribution to purine salvage and β-lactam resistance, particularly
451 if they are differentially regulated under specific growth conditions. The *deoD1* gene
452 is co-located on the chromosome with a major facilitator superfamily (Mfs) gene,
453 *deoC1* (deoxyribose-phosphate aldolase) and *deoB* (phosphopentomutase), which
454 may be expressed as an operon. Mutations in the Mfs gene, *deoC1* and *deoB* genes
455 alone were not associated with altered OX susceptibility (65). Nevertheless, DeoD1
456 activity may be dependent on the Mfs protein or a solute/ion transported by this
457 membrane protein. In contrast the *deoD2* gene is monocistronic and a second
458 deoxyribose-phosphate aldolase, *deoC2*, sharing 98% identity with *deoC1*, is
459 transcribed divergently from *deoD2*. The *purH* gene, which encodes the bifunctional
460 phosphoribosylaminoimidazolecarboxamide formyltransferase / IMP cyclohydrolase is
461 the penultimate gene in the *purEKCSQLFMNHD* operon followed only by *purD*. A *purD*
462 mutation, like all other *pur* operon mutations is accompanied by increased OX
463 resistance. PurH is responsible for the final step in the purine biosynthetic pathway,
464 converting 5-aminoimidazole-4-carboxamide ribonucleotide (AICAR) into IMP. AICAR
465 is produced by PurB, which is also part of the purine salvage pathway and *purB* can
466 be transcriptionally regulated independent of the *pur* operon (66). Unlike other Pur
467 enzymes, the bifunctional activity of PurH (synthesis and break-down of IMP),
468 combined with its requirement for AICAR from the *de novo* or purine salvage pathways
469 points to a complex role of this enzyme in purine metabolism and may suggest that its

470 impact on OX resistance is more dependent on growth conditions than other *pur*
471 operon enzymes.
472 Arising from studies to uncover the therapeutic potential of bactericidal and
473 bacteriostatic compounds produced by coagulase-negative staphylococci (CoNS) to
474 compete with *S. aureus* in shared ecological niche, the Heinrich's group identified the
475 CoNS-produced purine analogue 6-thioguanine (6-TG) and revealed its potential to
476 both inhibit growth of *S. aureus* by interfering with ribosome biogenesis and
477 downregulate *agr*-controlled virulence under purine limited growth conditions (67).
478 Resistance to 6-TG can arise through mutations in PbuG (also named StgP, 6-
479 thioguanine permease) and the Hpt hypoxanthine phosphoribosyltransferase (53),
480 demonstrating that guanine/6-TG are transported and metabolised by PbuG/StgP and
481 Hpt, respectively. We showed here that guanosine was unable to resensitize the 6-TG
482 resistant *hpt* mutants R10 and R11 (53) to OX, further supporting the role for Hpt in
483 guanine/6-TG metabolism. Our screen of suppressor mutants resistant to OX/Gua
484 combinations also identified stop codon mutations in *hpt* as well as *nupG*, *prs* and in
485 transcriptional (*rpoB*) and translational (tRNAs, ClpX) machinery genes. Interestingly,
486 while the R10 and R11 *hpt* mutants were resistant to guanosine/OX combinations,
487 they were susceptible to OX/Xan presumably because xanthosine is processed by the
488 Xpt phosphoribosyltransferase thus bypassing Hpt. On the other hand, the GS8 and
489 GS25 OX/Gua suppressor mutants carrying a Hpt L_{113}Stop mutation unexpectedly
490 remained resistant to OX/Xan. Although the reason for this difference is unclear, one
491 possibility is that Hpt also plays a role in processing xanthosine. If this is true, the Hpt
492 amino acid substitutions in R10 and R11 must interfere with guanosine processing,
493 but may not affect processing of xanthosine whereas the L_{113}Stop mutation
494 presumably blocks processing of both nucleosides. Interestingly, a M_1I mutation in *hpt*
495 likely to negatively impact translation initiation was previously implicated the HoR
496 phenotype (44). Similarly a *guaA* deletion mutation resulted in HoR resistance. There
497 are no transposon insertions in *hpt* or *guaA* in the NTML indicating that these genes
498 are important for growth under standard laboratory conditions. Collectively our data
499 are in keeping with previous studies indicating that mutations negatively impacting
500 GTP biosynthetic pathway enzyme activity are accompanied by increased resistance
501 to β-lactams and β-lactam/nucleoside combinations.

502 Our data showed that *nupG* and *deoD2* mutants significantly increased β-lactam
503 resistance independent of changes in PBP2a levels. Several lines of evidence support
504 the conclusion that purine homeostasis regulated β-lactam resistance is
505 mechanistically separate from PBP2a expression. For instance, our data showed that
506 guanosine also significantly reduces the OX MICs of a laboratory MSSA strain and the
507 NTML *mecA* transposon mutant. Two *clpX* stop codon mutations (G_{98}* and G_{278}*) were
508 also identified giving rise to resistance to OX/Gua and OX/Xan combinations, and very
509 high OX MICs. The ClpXP chaperone-protease complex is known to control β-lactam
510 resistance in MRSA (25, 26, 68), independent of changes in *mecA* transcription or
511 PBP2a levels (25). Here we also identified RpoB T_{480}K and T_{622}I substitutions
512 implicated in resistance to nucleoside/OX combinations. Two independent studies of
513 *rpoB* and *rpoC* mutations associated with high-level β-lactam resistance ruled out
514 changes in PBP2a expression (6, 62). In a recent analysis Giulieri et al (69) implicated
515 both *gdpP*/*dacA*-regulated c-di-AMP signal transduction, as well as the ClpXP
516 chaperone-protease complex in *mecA*-independent, low level OX resistance.
517 Collectively these findings support the conclusion that altered regulation of PBP2a
518 expression does not play an important role in the regulation of β-lactam susceptibility
519 by nucleoside/OX combinations. Instead our data showing that guanosine alone, and
520 in particular in combination with OX, significantly reduces c-di-AMP levels in a
521 NupG/DeoD2-dependent manner and dramatically increases cell size.
522 Osmoregulation and cell size are among the important phenotypes controlled by c-di-
523 AMP (23, 33) suggesting that deregulation of cellular osmotic control by exogenous
524 purine nucleosides is the most likely mechanism for increased β-lactam susceptibility.
525 From a therapeutic perspective, our *in vitro* kill curves revealed significant bactericidal
526 activity using combinations guanosine and OX at concentrations up to 128 μg/ml,
527 which are within the range of flucloxacillin intravenously administered to human
528 patients (100-200 mg/kg/day). While the emergence of OX/Gua suppressor mutants
529 appeared to be significantly reduced at higher oxacillin concentrations (as evidenced
530 by the absence of re-growth in kill curve cultures), this remains a potential barrier to
531 the use of nucleosides as β-lactam adjuvants. Future studies to measure the anti-
532 MRSA activity of different purine nucleosides or purine analogues in combination with
533 different β-lactams may identify more effective therapeutic regimes. Nevertheless,

534 drugs derived from purine and pyrimidine nucleotides are already used for the
535 treatment of cancer and viral infections highlighting the potential clinical applications
536 of these findings, not only for MRSA but also other pathogens on the World Health
537 Organisation's list of priority antibiotic-resistant pathogens. Using purine nucleosides
538 as adjuvants to increase the susceptibility of clinically important pathogens to β-
539 lactams has the potential to facilitate new treatments with lower antibiotic doses and
540 with drug combinations that are toxic at higher concentrations.
541

542 **Materials and Methods**

543 **Bacterial strains and growth conditions.**

544 Bacterial strains and plasmids used in this study are listed in Table S1. *Escherichia*
545 *coli* strains were grown in Luria Bertani (LB) broth or agar (LBA) and *Staphylococcus*
546 *aureus* strains were grown in Mueller-Hinton Broth (MHB), Mueller-Hinton Agar
547 (MHA), Tryptic Soy Broth (TSB), Tryptic Soy Agar (TSA), chemically defined medium
548 (CDM), supplemented with erythromycin (Erm) 10 μg/ml, chloramphenicol (Cm) 10
549 μg/ml, ampicillin (Amp) 100 μg/ml, kanamycin (Km) 90 μg/ml, guanosine , xanthosine
550 or adenosine (0.2 – 1 g/l) where indicated.
551 Data from growth experiments in a Tecan Sunrise microplate instrument were
552 recorded using Magellan software. Overnight cultures were grown in 5 ml TSB using
553 a single colony, and were washed once in PBS before being used to inoculate CDM
554 cultures. PBS washed overnight cultures were adjusted to an OD_{600} of 0.1 in PBS and
555 10 μl inoculated into 200 μl media per well before being incubated at 35°C for 24 h
556 with shaking and A_{600} recorded every 15 min intervals.
557 For flask growth curves, 250 ml flasks were filled with 25 ml growth media, and cultures
558 grown overnight in TSB were used to inoculate the media at a starting A_{600} of 0.01.
559 Flasks were incubated at 37°C shaking at 200 rpm. A_{600} readings were measured at
560 2 h intervals for 12 hours and an extra reading was taken at 24 hours.
561 Colony forming units (CFUs) were enumerated by serially diluting 100 μl aliquots
562 removed from flask cultures. Plates were incubated for 20 h at 37 °C and colonies
563 enumerated, and CFUs per ml suspension per OD_{600} calculated. Three independent

564 biological replicates were performed for each strain and the resulting data plotted
565 using GraphPad Prism software.

566 **Genetic manipulation of *S. aureus*.** Phage 80α was used as described previously
567 (70) to transduce the transposon insertions from NE650, NE1419 into the parent JE2
568 strain to rule out the possibility that uncharacterised mutations in the NTML mutants
569 may contribute to the increased antibiotic resistance phenotypes. Transposon
570 insertions were verified by PCR amplification of the target loci using primers listed in
571 Table S2.
572 To complement NE650 and NE1419, 1,387bp and 1,740bp PCR fragments were
573 amplified using JE2 gDNA as template and the primers INF_deoD_F / INF_deoD_R
574 and INF_nupG_F / INF_nupG_R, respectively (Table S2, Fig S4). The Clontech
575 Infusion Cloning kit was used to insert the fragments into the *Eco*R1 restriction site of
576 pLI50 to generate pLI50_*nupG,* and pLI50_*deoD2*. The recombinant plasmids were
577 first transformed into cold-competent *E. coli* HST08 before being transformed by
578 electroporation into the restriction-deficient *S. aureus* strain RN4220 and finally into
579 NE650 and NE1419.
580
581 **PBP2a Western blot analysis.** Single colonies from wild-type JE2, NE1419 (*nupG*),
582 NE650 (*deoD2*), NE1419 pLI50_*nupG*, NE650 pLI50_*deoD2*, MSSA strain 8325-4
583 (negative control) and HoR MRSA strain BH1CC (positive control) were inoculated in
584 MHB 2% NaCl overnight and grown at 35°C with 200 rpm shaking. All cultures were
585 supplemented with 5 μg/ml OX, with the exception of 8325-4 which was grown in MHB
586 2% NaCl without antibiotic and BHICC which was grown with 32 μg/ml OX. The next
587 day, samples were pelleted and resuspended in PBS to an A_{600} = 10. Six μl of
588 lysostaphin (10 μg/ml) and 1 μl of DNase (10 μg/ml) was added to 500 μl of this
589 concentrated cell suspension before being incubated at 37°C for 40 min. Next, 50 μl
590 of 10% SDS was added and the incubation continued for a further 20 min. The lysed
591 cells were then pelleted in a microcentrifuge for 15 min, following which the protein-
592 containing supernatant was collected and total protein concentration determined using
593 the Pierce BCA Protein Assay Kit. For each sample, 6 μg total protein was run on a
594 7.5% Tris-Glycine gel, transferred to a PVDF membrane and probed with anti-PBP2a

595 (1:1000), followed by HRP-conjugated protein G (1:2000) and colorimetric detection
596 with Opti-4CN Substrate kit. Three independent experiments were performed.
597
598 **Antibiotic disc diffusion susceptibility assays.** Disk diffusion susceptibility testing
599 was performed in accordance with Clinical Laboratory Standards Institute (CLSI)
600 guidelines (71) with the following modifications. Overnight cultures were diluted into
601 fresh TSB and grown for 3 h at 37 °C. Day cultures were then adjusted to A_{600} = 0.5
602 and 150 μl of this suspension was swabbed evenly 3 times across the surface of an
603 MHA plate (4 mm agar depth). 6 mm antibiotic discs were applied, before incubation
604 for times specified by CLSI guidelines for stated antibiotics at 35 - 37°C. Twenty μl of
605 guanosine at varying concentrations (50 - 750 μg/ml) was spotted onto discs to
606 demonstrate synergistic activity with β-lactam antibiotics where indicated. Three
607 independent measurements were performed for each strain.
608
609 **Antibiotic minimum inhibitory concentration (MIC) and synergy assays.** MIC
610 measurements by broth microdilutions were performed in accordance with CLSI
611 methods for dilution susceptibility testing of staphylococci (72) with modifications as
612 follows: guanosine, xanthosine or adenosine were supplemented into culture media at
613 concentrations ranging from 200 – 1000 μg/ml. Strains were first grown at 37 °C on
614 MHA (or MHB NaCl for OX MIC assays) for 24 h and 5 - 6 colonies were resuspended
615 in 0.85% saline before being adjusted to 0.5 McFarland standard (A_{600} = 0.01). The
616 cell suspension was then diluted 1:20 in PBS and 20 μl used to inoculate 180 μl MHB
617 / MHB NaCl supplemented with purines as indicated in the individual wells of 96-well
618 plates. The plates were incubated at 37 °C for 24 h and MIC values were recorded as
619 the lowest antibiotic concentration where no growth was observed.
620
621 **Isolation of suppressor mutants resistant to guanosine/oxacillin combination.**
622 Suppressor mutants were isolated from JE2 cultures serially passaged in MHB 2%
623 NaCl supplemented with 200 μg/ml guanosine and 32 μg/ml OX at 35°C. Using 96-
624 well plates, 100 μl of culture medium was inoculated with 2 - 8 x 10^5 CFU/ml from a
625 JE2 overnight culture and growth was monitored for 24 h in a Tecan Sunrise
626 microplate instrument using Magellan software, after which a 1:20 dilution was used
627 to inoculate 100 μl of the same medium in the corresponding well of a new plate, which

628 was incubated for a further 24 h. In wells showing visible growth, 5 μl of culture was
629 inoculated onto TSA plates to purify single colonies from the suppressor strains. The
630 susceptibility (MICs) of each of the isolated suppressor strains to OX and OX/GUA
631 combinations was confirmed as described above.
632
633 **Genomic DNA (gDNA) extraction and whole-genome sequencing (WGS).**
634 Genomic DNA (gDNA) extractions were performed using the Wizard® Genomic DNA
635 Purification Kit (Promega) following pre-treatment of *S. aureus* cells with 10 μg/ml
636 lysostaphin (Ambi Products LLC) at 37°C for 30 min. DNA libraries were prepared
637 using an Illumina Nextera DNA kit. An Illumina MiSeq v2 300 cycle kit was used for
638 the genome sequencing and the 150 bp paired end sequencing run was performed at
639 the MRC London Institute of Medical Sciences Genomics Facility. The CLC Genomics
640 Workbench software (Qiagen Version 20) was used for genome sequencing analysis
641 of the different strains, as described previously (39). As a reference genome, a contig
642 was produced for wild-type JE2 by mapping Illumina reads onto the closely related
643 USA300 FPR3757 genome sequence (RefSeq accession number NC_07793.1). The
644 Illumina short read sequences from NTML mutants of interest were then mapped onto
645 the assembled JE2 sequence, and the presence of the transposon insertion
646 confirmed. Single Nucleotide Polymorphisms (SNPs), deletions or insertions were
647 mapped to the genomes of the NTML mutants and OX/Gua resistant suppressor
648 strains and the presence of large deletions ruled out by manually searching for zero
649 coverage regions. Whole genome sequence data is available from the European
650 Nucleotide Archive (Study Accession number PRJEB55671), accession numbers
651 ERS13358424 - ERS13358446).
652 **Antibiotic kill curves**. Kill Curves were performed according to CLSI guidelines to
653 determine the extent of synergy between purines and oxacillin. Overnight cultures
654 grown in MHB NaCl were diluted 1:100 and allowed to grow for three hours
655 (exponential growth phase) before being inoculated into 25 ml of MHB NaCl in 250 ml
656 flasks at a starting cell density of approximately $1x10^6$ CFU/ml. The flasks were
657 incubated at 35°C with shaking at 200 rpm and CFUs were enumerated after 0, 2, 4,
658 6, 8, 12 and 24 h by serially diluting and plating 100 μl aliquots removed from flask
659 cultures on tryptone soya agar plates.

660
661 **Microscopy and cell size determination**. For microscopy experiments, MRSA strain
662 JE2 was grown overnight at 37°C in MHB. The next day, it was back-diluted into MHB,
663 MHB Gua 0.2 g/l, MHB OX 1 μg/ml and MHB Gua 0.2 g/l OX 1 μg/ml and day cultures
664 were grown for 5 hours at 35°C. After the 5-hour growth, the day cultures were washed
665 and normalized to an A_{600} of 1 in PBS and 75 μl of these cultures were double stained
666 for 30 mins at 37 °C with vancomycin-BODIPY FL at a final concentration of 2 μg/ml
667 and WGA Alexa Fluor 594 at a final concentration of 25 μg/ml. Bacteria were then
668 collected by centrifugation for 2 mins at 14,000 x*g*. The cells were resuspended with
669 100 μl of PBS, pH 7.4, and 5 μl of this sample was spotted onto a thin 1% agarose gel
670 patch prepared in PBS. Stained bacteria were then imaged at X1000 magnification
671 using Olympus LS FLUOVIEW Fv3000 Confocal Laser Scanning Microscope. Cell
672 size was measured as previously described (39) using ImageJ software. Images of
673 cells from three biological replicates were acquired, 40 cells measured per biological
674 replicate (120 cells in total per condition), and the average and standard deviations for
675 the three biological replicates were plotted using GraphPad Prism version 9.2 and
676 significant differences were determined using one-way ANOVA followed by Tukey's
677 post-hoc.
678
679 **GTP assays.** A GTPase-Glo bioluminescence assay kit (Promega) was used and the
680 manufacturer's guidelines were adjusted to measure relative intracellular GTP levels
681 by luminescence. Briefly overnight cultures of JE2, *nupG* and *deoD2* grown at 37°C in
682 MHB NaCl were used to inoculate duplicate MHB NaCl cultures supplemented with
683 guanosine (Gua, 0.2 g/l) and/or OX (OX, 1 μg/ml) at a starting A_{600} = 0.05 before these
684 were again incubated overnight at 37°C. Cell pellets were lysed and total protein
685 concentrations determined using a Bicinchoninic Acid (BCA) assay. The protein
686 concentration in each lysate was adjusted to 50 μg/ml and 2.5 μl (125 ng) used in each
687 GTPase-Glo assay.
688
689 **Measurement of (p)ppGpp.** Cultures of JE2, *nupG* and *deoD2* were grown overnight
690 at 37°C in MHB, followed by dilution in MHB NaCl with OX (1 μg/ml) and/or guanosine
691 (0.2 g/l) to A_{600} = 0.05. Cells were grown to A_{600} = 0.5 and divided into 2 aliquots. To
692 one, 3.7 MBq of $(^{32}P)H_3PO_4$ was added, while the other lacked radiation to allow for

693 normalization of cultures via protein concentrations by BCA assay. Both sets of culture
694 were grown overnight and the non-radioactive set used to determine protein
695 concentration. Radioactive culture corresponding to 150 ng of protein were lysed by
696 the addition of 2 M formic acid and subsequently subjected to four freeze/thaw cycles.
697 Ten μl of the supernatant fractions were subsequently spotted on PEI-cellulose F TLC
698 plates (Merck Millipore) and nucleotides separated using a 1.5 M KH_2PO_4, pH 3.6,
699 buffer. The radioactive spots were visualized using an FLA 7000 Typhoon
700 PhosphorImager, and data were quantified using ImageQuantTL software.
701
702 **Quantification of c-di-AMP levels using a competitive ELISA.** Relative intracellular
703 levels of c-di-AMP were determined using a previously described competitive ELISA
704 method (73) with some modifications. Briefly, single colonies of wild-type JE2, *nupG*
705 (NE1419) and *deoD2* (NE650) were picked from TSA plates and used to inoculate 5
706 ml or 12 ml of MHB 2% NaCl with or without guanosine (0.2 g/l) and/or OX (0.2 μg/ml)
707 and the cultures were incubated for 18 h at 37°C with shaking. The 5ml cultures were
708 grown in 20 ml tubes and 12 ml cultures were grown in 125 ml flasks. Next day, 1.5
709 ml (for all strains grown without OX), 3 ml (for *nupG* and *deoD2* grown in OX and the
710 wild-type grown in OX alone) or 6 ml (for wild-type JE2 grown in both OX and
711 guanosine) were collected by centrifugation, washed three times with PBS,
712 resuspended in 0.75 ml of 50 mM Tris pH 8 buffer supplemented with 20 ng/ml
713 lysostaphin and incubated for 1 h before completing cell lysis by bead beating.
714 Following centrifugation for 5 min at 17,000 ×*g*, the supernatant from the cell lysates
715 were transferred to new tubes and protein concentration of the samples was
716 determined using a Pierce BCA protein assay kit (Thermo Scientific, Waltham, MA,
717 USA). The samples were then heated to 95°C for 10 min, centrifuged for 5 min at
718 17,000 ×*g* and the supernatant containing c-di-AMP was transferred to a new tube.
719 The samples were diluted to a protein concentration of 300-800 μg/ml, as appropriate.
720 100 μl of coating buffer (50 mM Na_2C0_3, 50 mM $NaHCO_3$, pH 9.6) containing 10 μg/ml
721 of the c-di-AMP binding protein $CpaA_{SP}$ was aliquoted into each well of a 96 well
722 NUNC MaxiSorp plate (Thermo Scientific, Waltham, MA, USA), which was then
723 incubated for 18 h at 4°C. The plate was then washed three times with 200 μl PBST
724 pH 7.4 (10 mM Na_2HPO_4, 1.8 mM KH_2PO_4 137 mM NaCl, 2.7 mM KCl, 0.05% (v/v)

725 Tween 20), blocked for 1 h at 18°C with 150 μl blocking solution (1% BSA in PBS pH
726 7.4) and again washed three times with 200 μl PBST. 250 μl aliquots of the samples
727 (with three technical replicates for each biological replicate) or standards (two
728 technical replicates) were then mixed with 250 μl of a 50 nM biotinylated c-di-AMP
729 solution prepared in 50 mM Tris pH 8 buffer. For the standard curve, c-di-AMP
730 standards were prepared in 50 mM Tris pH 8 buffer at concentrations of 0, 12.5, 25,
731 37.5, 50, 75, 100 and 200 nM. Following the addition of the samples and the
732 standards, the 96 well plates were incubated for 2 h at 18°C and then washed three
733 times with PBST. Next, 100 μl of a high-sensitivity streptavidin-HRP solution (Thermo
734 Scientific, Waltham, MA, USA) diluted 1:500 in PBS was added to each well and the
735 plate was incubated for 1 h at 18°C. The plate was washed again three times with 200
736 μl PBST and 100 μl of a developing solution (0.103 M $NaHPO_4$, 0.0485 M citric acid,
737 500 mg/L o-phenylenediamine dihydrochloride, 0.03% H_2O_2) was added to each well
738 and the plate incubated for 15 min at 18°C. The reaction was stopped by adding 100
739 μl of 2 M H_2SO_4 solution and the absorbance measured in a plate reader at 490 nm.
740 c-di-AMP concentrations were calculated as ng c-di-AMP/mg protein. The data from
741 three independent experiments was collated and presented by showing relative c-di-
742 AMP levels in all samples compared to the wild-type grown in MHB NaCl, MHG NaCl
743 Ox or MHB NaCl Ox/Gua as appropriate, which was assigned a value of 100%.
744 Standard deviations are shown and significant differences were determined using one-
745 way ANOVA followed by Tukey's post-hoc tests.
746

Data availability

Whole genome sequence data is available from the European Nucleotide Archive (Study Accession number PRJEB55671), accession numbers ERS13358424 - ERS13358446. The SAUSA300_FRP3757 (TaxID:451515) reference genome sequence is available from NCBI.

Author contributions:

Aaron Nolan: Conceptualization, Formal analysis, Investigation, Methodology, Writing - original draft, Writing - review & editing

Merve S. Zeden: Conceptualization, Formal analysis, Investigation, Data curation, Methodology, Supervision, Writing - original draft, Writing - review & editing

Christopher Campbell: Conceptualization, Formal analysis, Investigation, Methodology, Writing - review & editing

Igor Kviatkovski: Formal analysis, Investigation, Methodology, Writing - review & editing

Lucy Urwin: Formal analysis, Investigation, Methodology, Writing - review & editing

Rebecca M. Corrigan: Funding acquisition, Formal analysis, Investigation, Methodology, Supervision, Writing - review & editing

Angelika Gründling: Funding acquisition, Formal analysis, Investigation, Methodology, Supervision, Writing - review & editing

James P. O'Gara: Conceptualization, Formal analysis, Funding acquisition, Project administration, Supervision, Writing - original draft, Writing - review & editing

Acknowledgements

A.N., M.S.Z., C.C. and J.P.O'G. were supported by grants from the Health Research Board (ILP-POR-2019-102) (www.hrb.ie), the Irish Research Council (GOIPG/2014/763) (www.research.ie) and Science Foundation Ireland (19/FFP/6441) (www.sfi.ie). L.U. and R.M.C. were supported by a Sir Henry Dale Fellowship jointly funded by the Wellcome Trust and the Royal Society (104110/Z/14/A). I.K. and A.G. were supported by Wellcome trust grant 210671/Z/18/Z/WT. We are grateful to Prof. David Heinrichs for the gift of strains *S. aureus* R10 and R11 and Dr. Peter Owens from the Centre for Microscopy & Imaging at the University of Galway (www.imaging.nuigalway.ie) for his scientific and technical assistance. The funders had no role in study design, data collection and interpretation, or the decision to submit the work for publication.

Tables

791 **Table 1.** Antibacterial activity (minimum inhibitory concentrations, MICs) of oxacillin (OX)
792 alone and in combination with guanosine (Gua), xanthosine (Xan) or adenosine (Ade) against
793 *S. aureus* strains, purine metabolism mutants, and *S. epidermidis* RP62A.

Strain	Oxacillin/Nucleoside combination				
	OX*	OX/Gua (0.2 g/l)**	OX/Gua (1 g/l)**	OX/Xan (1 g/l)**	OX/Ade (1 g/l)**
JE2	64	2-4	0.5-1	0.5-1	256
USA300	64	4-8	1-2	1-2	256
MW2	64	32	32	32	ND
DAR13	64	8	4-8	8	
DAR173	256	16	16	8	
DAR169	128	8-16	8-16	16	
DAR45	4	2	1	1	
DAR22	128	16	8	4-8	
S. epidermidis RP62A	128	8	4-8	32	ND
COL	512	512	256	256	ND
BH1CC	256	256	128	128	512
8325-4	0.125	0.06	0.03	0.06	0.25
NE1868 *mecA*	0.25	0.125	0.06	0.125	1
NE529 *purF*	128	8	1	0.5	256
NE522 *purA*	128	2	ND		
NE950 *purB*	128	4			
NE529 *purC*	128	4			
NE581 *purD*	128	4			
NE744 *purK*	128	2			
NE1785 *purN*	128	4			
NE1134 *purS*	128	8			
NE353 *purH*	64	8			
NE1101 *purM*	128	8			
NE1464 *purL*	128	8			
NE494 *purQ*	128	8			
NE1237 *purR*	32	4-8	1-2	0.5-1	64
NE1419 *nupG*	128	128	128	0.5-1	256
NE283 *pbuG*	128	4	2	0.5	256
NE280 *pbuX*	256	4-8	2	256	256
NE650 *deoD2*	128	128	128	0.5-1	256
NE477 *deoD1*	64	1	0.5-1	0.5-1	256
USA300 R10 *hpt* $S_{71}C$	256	128	128	8	256
USA300 R11 *hpt* $T_{61}P$	256	128	128	16	256
NE1419 pLI50_*nupG*	64	4-8	0.5	0.5	256
NE650 pLI50_*deoD2*	64	4-8	0.5	0.5	256
ANG3165 rsh_{syn}	128	4-8	1-2	0.5-1	256
ANG1961 Δ*gdpP*::Km	128	128	128	128	128
ANG3664 *dacA* $G_{206}S$	1	0.25	0.125	<0.125	16

794
795
796

797 * MIC values for OX in Mueller Hinton 2% NaCl broth (MHB); μg/ml
798 ** MIC values for OX in combination with guanosine (0.2 or 1 g/l), xanthosine (1 g/l) or
799 adenosine (1 g/l) in MHB, μg/ml
800 ‡ND. Not determined.
801

802 **Table 2.** Antibacterial activity (minimum inhibitory concentrations, MICs) of oxacillin (OX)
803 alone and in combination with guanosine (Gua) or xanthosine (Xan), against wild-type
804 MRSA and selected OX/Gua and OX (HoR) suppressor mutants.

Antibiotic → **↓ Strain**	OX[1]	OX/Gua (1 g/l)[2]	OX/Xan (1 g/l)[2]	Mutation(s)
Wild-type				
JE2	64	0.5-1	0.5-1	- [3]
OX/Gua suppressors				
GS1	256	256	128	ClpX, G_{278}Stop
GS3	256	128	128	tRNA-Met (RS09985)
GS4	256	256	128	RpoB, T_{480}K
GS6	256	256	128	tRNA-Met (RS09985)
GS8	256	256	128	Hpt, L_{113}Stop
GS10	256	256	128	RpoB, T_{622}I; tRNA-Leu (RS10005)
GS15	256	256	128	Prs, G_{35}D
GS16	256	256	128	Prs, G_{35}D; PdhB G_{65}V
GS17	256	128	128	RpoB, T_{622}I
GS21	256	128	128	tRNA-Ala (RS02670); tRNA-Met (RS09985)
GS22	256	256	128	Prs, G_{35}D; RS06410, G_{108}Stop
GS23	256	256	128	Prs, G_{35}D; PdhB G_{65}V
GS25	256	256	256	Hpt, L_{113}Stop
GS27	256	128	128	ClpX, G_{278}Stop; tRNA-Ala (RS02670)
GS28	256	256	128	RpoB, T_{622}I; NupG, W_{29}Stop; FemA, A_{344}T
GS29	256	128	128	RpoB, T_{480}K; Intergenic
OX suppressors (HoRs)				
OS14	128	256	256	ClpX, G_{98}Stop
OS18	128	64	32	RsbW, P_{101}H
OS26	128	4	4	PBP2, F_{44}S
OS30	128	64	32	RsbW, P_{101}H

805
806 [1] MICs for OX; μg/ml
807 [2] MICs for OX in combination with 1g/l guanosine or xanthosine; μg/ml
808 [3] A HemE L_{111}F mutation was identified in JE2 and all of the GS and OS suppressors
809 sequenced in this experiment.

810 **Figure legends**
811
812 **Fig. 1.** Overview of purine salvage and *de novo* biosynthetic pathways including
813 transporters and enzymes implicated in susceptibility to nucleoside/β-lactam
814 combinations. Inosine monophosphate (IMP) synthesized from ribose 5-P by enzymes
815 encoded by the *pur* operon can be fluxed to ATP and GTP. Nucleotides and
816 nucleosides can be transported into the cell via permeases including NupG, PbuX and
817 PbuG (StgP), where they can be salvaged and returned to the intracellular nucleotide
818 pool via the activity of enzymes including the nucleoside phosphorylases DeoD2
819 (SAUSA300_2091) and DeoD1 (SAUSA300_0138), hypoxanthine
820 phosphoribosyltransferase Hpt, xanthosine phosphoribosyltransferase Xpt and
821 adenosine phosphoribosyltransferase Apt. Mutations in *hpt*, *prs, guaB and guaA* have
822 previously been implicated in the high-level, homogeneous (HoR) β-lactam resistance
823 in MRSA (Dordel et al., 2014). GTP is a substrate for RelA, RelP and RelQ catalysed
824 synthesis of the stringent response alarmone (p)ppGpp. The cyclic dinucleotide
825 signalling molecule c-di-AMP is synthesized from ATP by DacA, and broken down by
826 GdpP, whose activity is repressed by ppGpp.
827
828 **Fig. 2. Exogenous guanosine only increases susceptibility of MRSA to β-**
829 **lactams and not other classes of antibiotic. A.** Susceptibility of wild-type JE2 to the
830 β-lactam antibiotics cefotaxime (top left), cefoxitin (top right), cefaclor (bottom left) and
831 penicillin G (bottom right) determined by disk diffusion assay on Mueller Hinton 2%
832 NaCl agar (MHA) (left), or MHA supplemented with 0.2 g/l guanosine (MHA Gua)
833 (right). This experiment was repeated three times and a representative image is
834 shown. **B.** Susceptibility of wild-type JE2 to the β-lactam antibiotics cefotaxime,
835 cefoxitin, cefaclor and penicillin G determined by disk diffusion assay on MHA or MHA
836 with 0.2 g/l guanosine (Gua). **C.** Susceptibility of wild-type JE2 to tetracycline,
837 vancomycin, chloramphenicol or gentamicin determined by disk diffusion assay on
838 MHA, or MHA with 0.2 g/l Gua. Data (zone diameters, mm) are the average of 3
839 independent experiments and error bars represent standard deviation. Statistical
840 significance was determined by one-way ANOVA. **** $p<0.0001$, ns, not significant
841

842 **Fig. 3. The *nupG* mutant NE1419 is more resistant to oxacillin and is not**
843 **susceptible to oxacillin-guanosine combinations. A.** Growth of wild-type and
844 NE1419 (*nupG*) for 24 hrs at 35°C in Mueller-Hinton 2% NaCl broth (MHB) and MHB
845 supplemented with oxacillin (OX) 1, 16 or 32 μg/ml. **B.** Growth of wild-type and
846 NE1419 (*nupG*) in MHB Gua 0.2g/l and MHB Gua 0.2 g/l supplemented with OX 1, 16
847 or 32 μg/ml. **C.** Growth of wild-type and NE1419 (*nupG*) in MHB Xan 0.2 g/l and MHB
848 Xan 0.2 g/l supplemented with OX 1, 16 or 32 μg/ml. **D.** Growth of wild-type and
849 NE1419 (*nupG*) in MHB Ade 0.2 g/l and MHB Ade 0.2 g/l supplemented with OX 1, 16
850 or 32 μg/ml. Growth (OD_{600}) was measured at 15 min intervals in a Tecan plate reader.
851 Data are the average of 3 independent experiments and error bars represent standard
852 deviation.
853
854 **Fig. 4. Exogenous guanosine, xanthosine and adenosine impact growth and**
855 **oxacillin susceptibility in a NupG-dependent manner.** Growth of wild-type and
856 NE1419 (*nupG*) at 35°C in Mueller-Hinton 2% NaCl broth (MHB) or MHB
857 supplemented with 0.2 g/l guanosine (Gua), Xanthosine (Xan) or adenosine (Ade) was
858 compared by measuring cell density (OD_{600}) **(A and C)** or enumerating colony forming
859 units (CFU/ml) **(B and D)** after 0, 2, 4, 6, 8, 12 and 24 h. Both strains were grown in
860 25 ml culture volumes in 250 ml flasks (1:10 ratio). Data are the average of 3
861 independent experiments and error bars represent standard deviation.
862
863 **Fig. 5. MRSA cell size is dramatically increased by growth in exogenous**
864 **guanosine and oxacillin. A.** Representative microscopic images of JE2 cells grown
865 in MHB NaCl or MHB NaCl supplemented with guanosine (Gua, 0.2 g/l), oxacillin
866 (OX,1 μg/ml) or a combination of Gua and OX labelled with vancomycin BODIPY FL
867 (green, top panel) or WGA Alexa Fluor 594 (red, bottom panel). **B.** Average diameter
868 of JE2 cells grown in MHB NaCl or MHB NaCl supplemented with Gua (0.2 g/l), OX (1
869 μg/ml) or a combination of Gua and OX. Images of cells from three biological replicates
870 were acquired using Fv3000 confocal microscope and software, 40 cells measured
871 per biological replicate (120 cells in total per condition), and the average and standard
872 deviations for the three biological replicates were plotted using GraphPad Prism V9.
873 Asterisks indicate statistically significant difference according to one-way ANOVA

874 followed by Tukey's multiple comparison post-hoc test (* $p<0.05$, ** $p<0.01$, ***
875 $p<0.001$, **** $p<0.0001$). Error bars indicate standard deviation.
876
877 **Fig. 6. Exogenous guanosine controls c-di-AMP in a *nupG* and *deoD2*-**
878 **dependent manner. A.** Relative c-di-AMP levels in wild-type, *nupG* and *deoD2* grown
879 for 18 h in 5 ml cultures with and without 0.2 g/l guanosine (Gua). **B.** Relative c-di-
880 AMP levels in wild-type grown for 18 h in 12 ml cultures with and without 0.2 μg/ml
881 oxacillin (Ox) and/or 0.2 g/l Gua. **C.** Relative c-di-AMP levels in wild-type, *nupG* and
882 *deoD2* grown for 18 h in 12 ml cultures with and without 0.2 μg/ml Ox and/or 0.2 g/l
883 Gua. Relative c-di-AMP levels are the averages of nine biological replicates from a
884 combination of three separate experiments with three bio-replicates each, normalized
885 as % relative to wild-type. Asterisks indicate statistically significant difference
886 according to one-way ANOVA followed by Tukey's multiple comparison post-hoc test
887 (* $p<0.05$, ** $p<0.01$, *** $p<0.001$, **** $p<0.0001$). Error bars indicate standard
888 deviation.
889
890

Supplementary Tables

903 **Table S1.** Bacterial strains and plasmids used in this study
904

Strains/plasmids	Relevant Details
JE2	USA300 cured of p01 & p03. Parent of Nebraska Transposon Mutant Library (NTML).
USA300 FPR3757	Community associated MRSA isolate (14). SCC*mec* type IV. CC8.
MW2	MRSA SCC*mec* type IV; CC1 (74)
DAR13	MRSA reference isolate; SCC*mec* type IV; CC8 (75, 76)
DAR173	MRSA reference isolate; SCC*mec* type IV; CC5 (75, 76)
DAR169	MRSA reference strain; SCCmec type I; CC8 (75, 76)
DAR45	MRSA reference isolate; SCC*mec* type II; CC30 (75, 76)
DAR22	MRSA reference isolate; SCC*mec* type III; CC5 (75, 76)
S. epidermidis RP62A	ATCC 35984. Methicillin resistant, biofilm positive (77)
COL	MRSA reference strain; SCC*mec* type I; CC8 (78)
BH1CC	MRSA clinical isolate; SCC*mec* type II; CC8 (75)
8325-4	NCTC 8325 derivative cured of prophages (79), MSSA, CC8.
NE1868 *mecA*	JE2 *mecA*. Erm^r. (52)
NE477 *deoD1*	JE2 *deoD1* (SAUSA300_0138). Erm^r. (52)
NE529 *purF*	JE2 *purF*. Erm^r. (52)
NE522 *purA*	JE2 *purA*. Erm^r. (52)
NE950 *purB*	JE2 *purB*. Erm^r. (52)
NE529 *purC*	JE2 *purC*. Erm^r. (52)
NE581 *purD*	JE2 *purD*. Erm^r. (52)
NE744 *purK*	JE2 *purK*. Erm^r. (52)
NE1785 *purN*	JE2 *purN*. Erm^r. (52)
NE1134 *purS*	JE2 *purS*. Erm^r. (52)
NE353 *purH*	JE2 *purH*. Erm^r. (52)
NE1101 *purM*	JE2 *purM*. Erm^r. (52)
NE1464 *purL*	JE2 *purL*. Erm^r. (52)
NE494 *purQ*	JE2 *purQ*. Erm^r. (52)
NE1237 *purR*	JE2 *purR*. Erm^r. (52)
NE1419 *nupG*	JE2 *nupG* (SAUSA300_0611). Erm^r. (52)
NE283 *pbuG/stgP*	JE2 *pbuG/stgP* (SAUSA300_2207). Erm^r. (52)
NE280 *pbuX*	JE2 *pbuX* (SAUSA300_0387). Erm^r. (52)
NE650 *deoD2*	JE2 *deoD2* (SAUSA300_2091). Erm^r. (52)
NE477 *deoD1*	JE2 *deoD1* (SAUSA300_0138). Erm^r. (52)
USA300 R10 *hpt* $S_{71}C$	USA300 6-thioguanine resistant mutant. Hpt $S_{71}C$ mutation (53)
USA300 R11 *hpt* $T_{61}P$	USA300 6-thioguanine resistant mutant. Hpt $T_{61}P$ mutation (53)
NE1419 pLI50_*nupG*	NE1419 pLI50_*nupG* Erm^r, Cm^r
NE650 pLI50_*deoD2*	NE650 pLI50_*deoD2*. Erm^r, Cm^r
ANG3165 rsh_{syn}	USA300 LAC*rsh_{syn}. (33)
ANG1961 Δ*gdpP*::Km	USA300 LAC*Δ*gdpP*::*kan.* Kan^r. (23)
ANG3664 *dacA* $G_{206}S$	USA300 *dacA* $G_{206}S$. (61)
nupG::Tn	*nupG*::Erm^r from NE1419 transduced into wild-type JE2
deoD2::Tn	*deoD2*::Erm^r from NE1419 transduced into wild-type JE2
MW2 *nupG*::Tn	*nupG*::Erm^r from NE1419 transduced into MW2
MW2 *deoD2*::Tn	*deoD2*::Erm^r from NE650 transduced into MW2
RN4220	Restriction deficient derivative of *S. aureus* 8325 (79)
E. coli HST08	TaKaRa *E. coli* HST08 Premium Electro-Cells
HST06 pLI50_*deoD2*	*E. coli* HST06 carrying pLI50_*deoD2*. Amp^r
HST06 pLI50_*nupG*	*E. coli* HST06 carrying pLI50_*nupG*. Amp^r

Plasmids	
pLI50	*E. coli* (Ap^r)-*Staphylococcus* (Cm^r)shuttle vector.
pLI50_*deoD2*	pLI50 carrying *deoD2* from JE2. Cm^r. This study.
pLI50_*nupG*	pLI50 carrying *nupG* from JE2. Cm^r. This study.

905
906
907
908
909 **Table S2.** Oligonucleotide primers used in this study.
910

Target gene	Primer name	Primer sequence (5'-3')
purA	purA_Tn_check	TCATCAATCGTAGTAGTTGGGACACA
purB	purB_Tn_check	GGAGAAGTAAAGTGAATAAATTCTGGTA
purC	purC_Tn_check	CCACTAGCAATATTACGAACAACTACTTC
purD	purD_Tn_check	GTCATTAGCGAGAACTCTTCACC
purF	purF_Tn_check	CGAAGAATGTGGCGTGTTTGG
purH	purH_Tn_check	CGCTTCATCATATTCTGCAGTATGC
purK	purK_Tn_check	CTGAAGATTGTCCATGTAGATACGTTGC
purL	purL_Tn_check	CGTACTACCGATGCTTGAAGTCCT
purM	purM_Tn_check	GCAAATCCAGCTACATCATATTCGC
purQ	purQ_Tn_check	CCAGGTTCGAATTGTGATAGAGACA
purS	purS_Tn_check	GGATGAAATATCTCCAGATACATGTCG
purN	purN_Tn_check	CACGCGCTTTGAAGATTTTAGCAGAAC
deoD1	deoD1_Tn_check	GAAGCAATTGGCGCAAAATGAC
deoD2	deoD2_Tn_check	CACCACATATTAACCAAATGGAG
nupG	nupG_Tn_check	GAGCAGCCAATGGTATCGCT
pbuX	pbuX_Tn_check	GGGAGAAGAATAATGAAAAATTTAATCC
pbuG	pbuG_Tn_check	CTGCACTTGTTACAACAGCGATTAACGG
relA	relA_Tn_check	GCGAGTGATGTTATTGAGTTGCC
Infusion cloning primers		
deoD2	INF_deoD2_F	TCGTCTTCAAGAATTACATGCGTTGGATTCACACA
	INF_deoD2_R	TACCGAGCTCGAATTTGGTAATGCTGGCGATGATG
nupG	INF_nupG_F	TCGTCTTCAAGAATTGGTAACAGGTAAAGGTACGCA
	INF_nupG_R	TACCGAGCTCGAATTATAGACGACATGCCTGGACA

911

References

1. Lowy FD. 1998. Staphylococcus aureus infections. N Engl J Med 339:520-32.
2. Martins A, Cunha Mde L. 2007. Methicillin resistance in Staphylococcus aureus and coagulase-negative staphylococci: epidemiological and molecular aspects. Microbiol Immunol 51:787-95.
3. van Hal SJ, Jensen SO, Vaska VL, Espedido BA, Paterson DL, Gosbell IB. 2012. Predictors of mortality in Staphylococcus aureus Bacteremia. Clin Microbiol Rev 25:362-86.
4. Liu C, Bayer A, Cosgrove SE, Daum RS, Fridkin SK, Gorwitz RJ, Kaplan SL, Karchmer AW, Levine DP, Murray BE, M JR, Talan DA, Chambers HF. 2011. Clinical practice guidelines by the infectious diseases society of america for the treatment of methicillin-resistant Staphylococcus aureus infections in adults and children: executive summary. Clin Infect Dis 52:285-92.
5. Hiramatsu K, Ito T, Tsubakishita S, Sasaki T, Takeuchi F, Morimoto Y, Katayama Y, Matsuo M, Kuwahara-Arai K, Hishinuma T, Baba T. 2013. Genomic Basis for Methicillin Resistance in Staphylococcus aureus. Infect Chemother 45:117-36.
6. Panchal VV, Griffiths C, Mosaei H, Bilyk B, Sutton JAF, Carnell OT, Hornby DP, Green J, Hobbs JK, Kelley WL, Zenkin N, Foster SJ. 2020. Evolving MRSA: High-level beta-lactam resistance in Staphylococcus aureus is associated with RNA Polymerase alterations and fine tuning of gene expression. PLoS Pathog 16:e1008672.
7. Bruniera FR, Ferreira FM, Saviolli LR, Bacci MR, Feder D, da Luz Gonçalves Pedreira M, Sorgini Peterlini MA, Azzalis LA, Campos Junqueira VB, Fonseca FL. 2015. The use of vancomycin with its therapeutic and adverse effects: a review. Eur Rev Med Pharmacol Sci 19:694-700.
8. Rybak MJ, Lomaestro BM, Rotscahfer JC, Moellering RC, Jr., Craig WA, Billeter M, Dalovisio JR, Levine DP. 2009. Vancomycin Therapeutic Guidelines: A Summary of Consensus Recommendations from the Infectious Diseases Society of America, the American Society of Health-System Pharmacists, and the Society of Infectious Diseases Pharmacists. Clinical Infectious Diseases 49:325-327.
9. Lamp KC, Rybak MJ, Bailey EM, Kaatz GW. 1992. In vitro pharmacodynamic effects of concentration, pH, and growth phase on serum bactericidal activities of daptomycin and vancomycin. Antimicrobial agents and chemotherapy 36:2709-2714.
10. Howe RA, Monk A, Wootton M, Walsh TR, Enright MC. 2004. Vancomycin susceptibility within methicillin-resistant Staphylococcus aureus lineages. Emerging infectious diseases 10:855-857.
11. Mwangi MM, Wu SW, Zhou Y, Sieradzki K, de Lencastre H, Richardson P, Bruce D, Rubin E, Myers E, Siggia ED, Tomasz A. 2007. Tracking the *in vivo* evolution of multidrug resistance in Staphylococcus aureus by whole-genome sequencing. Proceedings of the National Academy of Sciences of the United States of America 104:9451-9456.
12. Chambers HF. 2001. Methicillin-resistant Staphylococcus aureus. Mechanisms of resistance and implications for treatment. Postgrad Med 109:43-50.
13. Hartman BJ, Tomasz A. 1984. Low-affinity penicillin-binding protein associated with beta-lactam resistance in Staphylococcus aureus. J Bacteriol 158:513-6.
14. Diep BA, Gill SR, Chang RF, Phan TH, Chen JH, Davidson MG, Lin F, Lin J, Carleton HA, Mongodin EF, Sensabaugh GF, Perdreau-Remington F. 2006. Complete genome sequence of USA300, an epidemic clone of community-acquired meticillin-resistant Staphylococcus aureus. Lancet 367:731-9.
15. Francis JS, Doherty MC, Lopatin U, Johnston CP, Sinha G, Ross T, Cai M, Hansel NN, Perl T, Ticehurst JR, Carroll K, Thomas DL, Nuermberger E, Bartlett JG. 2005. Severe community-onset pneumonia in healthy adults caused by methicillin-resistant

964 *Staphylococcus aureus* carrying the Panton-Valentine leukocidin genes. Clin Infect
965 Dis 40:100-7.
966 16. Katayama Y, Ito T, Hiramatsu K. 2000. A new class of genetic element,
967 staphylococcus cassette chromosome mec, encodes methicillin resistance in
968 Staphylococcus aureus. Antimicrob Agents Chemother 44:1549-55.
969 17. Llarrull LI, Fisher JF, Mobashery S. 2009. Molecular basis and phenotype of
970 methicillin resistance in Staphylococcus aureus and insights into new beta-lactams
971 that meet the challenge. Antimicrob Agents Chemother 53:4051-63.
972 18. Finan JE, Rosato AE, Dickinson TM, Ko D, Archer GL. 2002. Conversion of oxacillin-
973 resistant staphylococci from heterotypic to homotypic resistance expression.
974 Antimicrob Agents Chemother 46:24-30.
975 19. Tomasz A, Nachman S, Leaf H. 1991. Stable classes of phenotypic expression in
976 methicillin-resistant clinical isolates of staphylococci. Antimicrobial agents and
977 chemotherapy 35:124-129.
978 20. Kim C, Mwangi M, Chung M, Milheirico C, de Lencastre H, Tomasz A. 2013. The
979 mechanism of heterogeneous beta-lactam resistance in MRSA: key role of the
980 stringent stress response. PLoS One 8:e82814.
981 21. Mwangi MM, Kim C, Chung M, Tsai J, Vijayadamodar G, Benitez M, Jarvie TP, Du L,
982 Tomasz A. 2013. Whole-genome sequencing reveals a link between beta-lactam
983 resistance and synthetases of the alarmone (p)ppGpp in Staphylococcus aureus.
984 Microb Drug Resist 19:153-9.
985 22. Pozzi C, Waters EM, Rudkin JK, Schaeffer CR, Lohan AJ, Tong P, Loftus BJ, Pier
986 GB, Fey PD, Massey RC, O'Gara JP. 2012. Methicillin resistance alters the biofilm
987 phenotype and attenuates virulence in Staphylococcus aureus device-associated
988 infections. PLoS Pathog 8:e1002626.
989 23. Corrigan RM, Abbott JC, Burhenne H, Kaever V, Gründling A. 2011. c-di-AMP is a
990 new second messenger in Staphylococcus aureus with a role in controlling cell size
991 and envelope stress. PLoS Pathog 7:e1002217.
992 24. Griffiths JM, O'Neill AJ. 2012. Loss of function of the *gdpP* protein leads to joint beta-
993 lactam/glycopeptide tolerance in Staphylococcus aureus. Antimicrob Agents
994 Chemother 56:579-81.
995 25. Baek KT, Gründling A, Mogensen RG, Thogersen L, Petersen A, Paulander W,
996 Frees D. 2014. beta-Lactam resistance in methicillin-resistant Staphylococcus
997 aureus USA300 is increased by inactivation of the ClpXP protease. Antimicrob
998 Agents Chemother 58:4593-603.
999 26. Jensen C, Baek KT, Gallay C, Thalso-Madsen I, Xu L, Jousselin A, Ruiz Torrubia F,
1000 Paulander W, Pereira AR, Veening JW, Pinho MG, Frees D. 2019. The ClpX
1001 chaperone controls autolytic splitting of Staphylococcus aureus daughter cells, but is
1002 bypassed by beta-lactam antibiotics or inhibitors of WTA biosynthesis. PLoS Pathog
1003 15:e1008044.
1004 27. Giuliani AL, Sarti AC, Di Virgilio F. 2019. Extracellular nucleotides and nucleosides
1005 as signalling molecules. Immunology Letters 205:16-24.
1006 28. Kilstrup M, Hammer K, Ruhdal Jensen P, Martinussen J. 2005. Nucleotide
1007 metabolism and its control in lactic acid bacteria. FEMS Microbiology Reviews
1008 29:555-590.
1009 29. Pesavento C, Hengge R. 2009. Bacterial nucleotide-based second messengers.
1010 Current Opinion in Microbiology 12:170-176.
1011 30. Gründling A, Lee VT. 2016. Old concepts, new molecules and current approaches
1012 applied to the bacterial nucleotide signalling field. Philosophical Transactions of the
1013 Royal Society B: Biological Sciences 371:20150503.

1014 31. Dengler V, McCallum N, Kiefer P, Christen P, Patrignani A, Vorholt JA, Berger-Bachi
1015 B, Senn MM. 2013. Mutation in the C-di-AMP cyclase *dacA* affects fitness and
1016 resistance of methicillin resistant Staphylococcus aureus. PLoS One 8:e73512.
1017 32. Fahmi T, Port GC, Cho KH. 2017. c-di-AMP: An Essential Molecule in the Signaling
1018 Pathways that Regulate the Viability and Virulence of Gram-Positive Bacteria. Genes
1019 (Basel) 8.
1020 33. Corrigan RM, Bowman L, Willis AR, Kaever V, Gründling A. 2015. Cross-talk
1021 between two nucleotide-signaling pathways in Staphylococcus aureus. J Biol Chem
1022 290:5826-39.
1023 34. Li L, Abdelhady W, Donegan NP, Seidl K, Cheung A, Zhou Y-F, Yeaman MR, Bayer
1024 AS, Xiong YQ. 2018. Role of Purine Biosynthesis in Persistent Methicillin-Resistant
1025 Staphylococcus aureus Infection. The Journal of infectious diseases 218:1367-1377.
1026 35. Li L, Li Y, Zhu F, Cheung AL, Wang G, Bai G, Proctor RA, Yeaman MR, Bayer AS,
1027 Xiong YQ. 2021. New Mechanistic Insights into Purine Biosynthesis with Second
1028 Messenger c-di-AMP in Relation to Biofilm-Related Persistent Methicillin-Resistant
1029 Staphylococcus aureus Infections. mBio 12:e0208121-e0208121.
1030 36. Lan L, Cheng A, Dunman PM, Missiakas D, He C. 2010. Golden pigment production
1031 and virulence gene expression are affected by metabolisms in Staphylococcus
1032 aureus. J Bacteriol 192:3068-77.
1033 37. Stulke J, Kruger L. 2020. Cyclic di-AMP Signaling in Bacteria. Annu Rev Microbiol
1034 74:159-179.
1035 38. Schuster CF, Bellows LE, Tosi T, Campeotto I, Corrigan RM, Freemont P, Gründling
1036 A. 2016. The second messenger c-di-AMP inhibits the osmolyte uptake system
1037 OpuC in Staphylococcus aureus. Sci Signal 9:ra81.
1038 39. Zeden MS, Schuster CF, Bowman L, Zhong Q, Williams HD, Gründling A. 2018.
1039 Cyclic di-adenosine monophosphate (c-di-AMP) is required for osmotic regulation in
1040 Staphylococcus aureus but dispensable for viability in anaerobic conditions. J Biol
1041 Chem 293:3180-3200.
1042 40. Corrigan RM, Gründling A. 2013. Cyclic di-AMP: another second messenger enters
1043 the fray. Nat Rev Microbiol 11:513-24.
1044 41. Aedo S, Tomasz A. 2016. Role of the Stringent Stress Response in the Antibiotic
1045 Resistance Phenotype of Methicillin-Resistant Staphylococcus aureus. Antimicrob
1046 Agents Chemother 60:2311-7.
1047 42. Geiger T, Goerke C, Fritz M, Schafer T, Ohlsen K, Liebeke M, Lalk M, Wolz C. 2010.
1048 Role of the (p)ppGpp synthase RSH, a RelA/SpoT homolog, in stringent response
1049 and virulence of Staphylococcus aureus. Infect Immun 78:1873-83.
1050 43. Lemos JA, Lin VK, Nascimento MM, Abranches J, Burne RA. 2007. Three gene
1051 products govern (p)ppGpp production by Streptococcus mutans. Mol Microbiol
1052 65:1568-81.
1053 44. Dordel J, Kim C, Chung M, Pardos de la Gándara M, Holden MT, Parkhill J, de
1054 Lencastre H, Bentley SD, Tomasz A. 2014. Novel determinants of antibiotic
1055 resistance: identification of mutated loci in highly methicillin-resistant subpopulations
1056 of methicillin-resistant Staphylococcus aureus. mBio 5:e01000.
1057 45. Martín-Rodríguez AJ, Römling U. 2017. Nucleotide Second Messenger Signaling as
1058 a Target for the Control of Bacterial Biofilm Formation. Curr Top Med Chem.
1059 46. Liu A, Tran L, Becket E, Lee K, Chinn L, Park E, Tran K, Miller JH. 2010. Antibiotic
1060 sensitivity profiles determined with an Escherichia coli gene knockout collection:
1061 generating an antibiotic bar code. Antimicrobial agents and chemotherapy 54:1393-
1062 1403.
1063 47. Blair JMA, Webber MA, Baylay AJ, Ogbolu DO, Piddock LJV. 2015. Molecular
1064 mechanisms of antibiotic resistance. Nature Reviews Microbiology 13:42-51.

1065 48. Turner NA, Sharma-Kuinkel BK, Maskarinec SA, Eichenberger EM, Shah PP,
1066 Carugati M, Holland TL, Fowler VG. 2019. Methicillin-resistant Staphylococcus
1067 aureus: an overview of basic and clinical research. Nature Reviews Microbiology
1068 17:203-218.
1069 49. Worthington RJ, Melander C. 2013. Combination approaches to combat multidrug-
1070 resistant bacteria. Trends in biotechnology 31:177-184.
1071 50. Waters EM, Rudkin JK, Coughlan S, Clair GC, Adkins JN, Gore S, Xia G, Black NS,
1072 Downing T, O'Neill E, Kadioglu A, O'Gara JP. 2017. Redeploying beta-lactam
1073 antibiotics as a novel antivirulence strategy for the treatment of methicillin-resistant
1074 Staphylococcus aureus infections. J Infect Dis 215:80-87.
1075 51. Plata KB, Riosa S, Singh CR, Rosato RR, Rosato AE. 2013. Targeting of PBP1 by
1076 beta-lactams determines *recA*/SOS response activation in heterogeneous MRSA
1077 clinical strains. PLoS One 8:e61083.
1078 52. Fey PD, Endres JL, Yajjala VK, Widhelm TJ, Boissy RJ, Bose JL, Bayles KW. 2013.
1079 A genetic resource for rapid and comprehensive phenotype screening of
1080 nonessential *Staphylococcus aureus* genes. mBio 4:e00537-12.
1081 53. Chin D, Goncheva MI, Flannagan RS, Heinrichs DE. 2021. Mutations in a Membrane
1082 Permease or *hpt* Lead to 6-Thioguanine Resistance in Staphylococcus aureus.
1083 Antimicrob Agents Chemother 65:e0076021.
1084 54. Salamaga B, Kong L, Pasquina-Lemonche L, Lafage L, von Und Zur Muhlen M,
1085 Gibson JF, Grybchuk D, Tooke AK, Panchal V, Culp EJ, Tatham E, O'Kane ME,
1086 Catley TE, Renshaw SA, Wright GD, Plevka P, Bullough PA, Han A, Hobbs JK,
1087 Foster SJ. 2021. Demonstration of the role of cell wall homeostasis in
1088 Staphylococcus aureus growth and the action of bactericidal antibiotics. Proc Natl
1089 Acad Sci U S A 118.
1090 55. Aiba Y, Katayama Y, Hishinuma T, Murakami-Kuroda H, Cui L, Hiramatsu K. 2013.
1091 Mutation of RNA polymerase β-subunit gene promotes heterogeneous-to-
1092 homogeneous conversion of β-lactam resistance in methicillin-resistant
1093 Staphylococcus aureus. Antimicrob Agents Chemother 57:4861-71.
1094 56. Gao W, Cameron DR, Davies JK, Kostoulias X, Stepnell J, Tuck KL, Yeaman MR,
1095 Peleg AY, Stinear TP, Howden BP. 2012. The RpoB H481Y Rifampicin Resistance
1096 Mutation and an Active Stringent Response Reduce Virulence and Increase
1097 Resistance to Innate Immune Responses in Staphylococcus aureus. The Journal of
1098 Infectious Diseases 207:929-939.
1099 57. Gao W, Cameron DR, Davies JK, Kostoulias X, Stepnell J, Tuck KL, Yeaman MR,
1100 Peleg AY, Stinear TP, Howden BP. 2013. The RpoB H(4)(8)(1)Y rifampicin
1101 resistance mutation and an active stringent response reduce virulence and increase
1102 resistance to innate immune responses in Staphylococcus aureus. J Infect Dis
1103 207:929-39.
1104 58. Johnson S, Krüger D, Labischinski H. 1995. FemA of Staphylococcus aureus:
1105 isolation and immunodetection. FEMS Microbiol Lett 132:221-8.
1106 59. Vilhelmsson O, Miller KJ. 2002. Synthesis of pyruvate dehydrogenase in
1107 Staphylococcus aureus is stimulated by osmotic stress. Appl Environ Microbiol
1108 68:2353-8.
1109 60. Li L, Cheung A, Bayer AS, Chen L, Abdelhady W, Kreiswirth BN, Yeaman MR, Xiong
1110 YQ. 2016. The Global Regulon sarA Regulates beta-Lactam Antibiotic Resistance in
1111 Methicillin-Resistant Staphylococcus aureus In Vitro and in Endovascular Infections.
1112 J Infect Dis 214:1421-1429.
1113 61. Bowman L, Zeden MS, Schuster CF, Kaever V, Gründling A. 2016. New Insights into
1114 the Cyclic Di-adenosine Monophosphate (c-di-AMP) Degradation Pathway and the
1115 Requirement of the Cyclic Dinucleotide for Acid Stress Resistance in Staphylococcus
1116 aureus. J Biol Chem 291:26970-26986.

1117 62. Boonsiri T, Watanabe S, Tan X-E, Thitiananpakorn K, Narimatsu R, Sasaki K,
1118 Takenouchi R, Sato'o Y, Aiba Y, Kiga K, Sasahara T, Taki Y, Li F-Y, Zhang Y, Azam
1119 AH, Kawaguchi T, Cui L. 2020. Identification and characterization of mutations
1120 responsible for the β-lactam resistance in oxacillin-susceptible mecA-positive
1121 Staphylococcus aureus. Scientific Reports 10:16907.
1122 63. Sause WE, Balasubramanian D, Irnov I, Copin R, Sullivan MJ, Sommerfield A, Chan
1123 R, Dhabaria A, Askenazi M, Ueberheide B, Shopsin B, Bakel Hv, Torres VJ. 2019.
1124 The purine biosynthesis regulator PurR moonlights as a virulence regulator in
1125 Staphylococcus aureus. Proceedings of the National Academy of Sciences
1126 116:13563-13572.
1127 64. Goncheva MI, Flannagan RS, Sterling BE, Laakso HA, Friedrich NC, Kaiser JC,
1128 Watson DW, Wilson CH, Sheldon JR, McGavin MJ, Kiser PK, Heinrichs DE. 2019.
1129 Stress-induced inactivation of the Staphylococcus aureus purine biosynthesis
1130 repressor leads to hypervirulence. Nat Commun 10:775.
1131 65. Gallagher LA, Shears R, Fingleton C, Alvarez L, M. WE, Clarke J, Bricio-Moreno L,
1132 Campbell C, Yadav A, Razvi F, O'Neill E, Cava F, O'Neill AJ, Fey PD, Kadioglu A,
1133 O'Gara JP. 2019. Impaired alanine transport or exposure to D-cycloserine increases
1134 the susceptibility of MRSA to beta-lactam antibiotics. bioRxiv 616920 doi:
1135 https://doi.org/10.1101/616920). .
1136 66. Gélinas M, Museau L, Milot A, Beauregard PB. 2020. Cellular adaptation and the
1137 importance of the purine biosynthesis pathway during biofilm formation in Gram-
1138 positive pathogens. bioRxiv doi:10.1101/2020.12.11.422287:2020.12.11.422287.
1139 67. Chin D, Goncheva MI, Flannagan RS, Deecker SR, Guariglia-Oropeza V, Ensminger
1140 AW, Heinrichs DE. 2021. Coagulase-negative staphylococci release a purine analog
1141 that inhibits Staphylococcus aureus virulence. Nat Commun 12:1887.
1142 68. Baek KT, Jensen C, Farha MA, Nielsen TK, Paknejadi E, Mebus VH, Vestergaard M,
1143 Brown ED, Frees D. 2021. A Staphylococcus aureus *clpX* Mutant Used as a Unique
1144 Screening Tool to Identify Cell Wall Synthesis Inhibitors that Reverse beta-Lactam
1145 Resistance in MRSA. Front Mol Biosci 8:691569.
1146 69. Giulieri SG, Guerillot R, Kwong JC, Monk IR, Hayes AS, Daniel D, Baines S, Sherry
1147 NL, Holmes NE, Ward P, Gao W, Seemann T, Stinear TP, Howden BP. 2020.
1148 Comprehensive Genomic Investigation of Adaptive Mutations Driving the Low-Level
1149 Oxacillin Resistance Phenotype in Staphylococcus aureus. mBio 11.
1150 70. Fingleton C, Zeden MS, Bueno E, Cava F, O'Gara JP. 2021. Mutation of lipoprotein
1151 processing pathway gene *lspA* or inhibition of LspA activity by
1152 globomycin increases MRSA resistance to β-lactam antibiotics. bioRxiv
1153 doi:10.1101/2021.02.03.429649:2021.02.03.429649.
1154 71. CLSI. 2018. Performance Standards for Antimicrobial Disk Susceptibility Tests;
1155 approved standard—12th ed. M02-A13., Wayne, PA.
1156 72. Wayne P. CLSI 2018. CLSI 2018. Performance standards for antimicrobial disk
1157 susceptibility tests. Approved standard, 12th ed. CLSI standard M02-A13. Clinical
1158 and Laboratory Standards Institute,.
1159 73. Underwood AJ, Zhang Y, Metzger DW, Bai G. 2014. Detection of cyclic di-AMP using
1160 a competitive ELISA with a unique pneumococcal cyclic di-AMP binding protein. J
1161 Microbiol Methods 107:58-62.
1162 74. Saiman L, O'Keefe M, Graham PL, 3rd, Wu F, Said-Salim B, Kreiswirth B, LaSala A,
1163 Schlievert PM, Della-Latta P. 2003. Hospital transmission of community-acquired
1164 methicillin-resistant Staphylococcus aureus among postpartum women. Clin Infect
1165 Dis 37:1313-9.
1166 75. O'Neill E, Pozzi C, Houston P, Smyth D, Humphreys H, Robinson DA, O'Gara JP.
1167 2007. Association between methicillin susceptibility and biofilm regulation in

1168 Staphylococcus aureus isolates from device-related infections. J Clin Microbiol
1169 45:1379-88.
1170 76. Robinson DA, Enright MC. 2003. Evolutionary models of the emergence of
1171 methicillin-resistant Staphylococcus aureus. Antimicrob Agents Chemother 47:3926-
1172 34.
1173 77. Conlon KM, Humphreys H, O'Gara JP. 2002. *icaR* encodes a transcriptional
1174 repressor involved in environmental regulation of ica operon expression and biofilm
1175 formation in Staphylococcus epidermidis. J Bacteriol 184:4400-8.
1176 78. Gill SR, Fouts DE, Archer GL, Mongodin EF, Deboy RT, Ravel J, Paulsen IT,
1177 Kolonay JF, Brinkac L, Beanan M, Dodson RJ, Daugherty SC, Madupu R, Angiuoli
1178 SV, Durkin AS, Haft DH, Vamathevan J, Khouri H, Utterback T, Lee C, Dimitrov G,
1179 Jiang L, Qin H, Weidman J, Tran K, Kang K, Hance IR, Nelson KE, Fraser CM. 2005.
1180 Insights on evolution of virulence and resistance from the complete genome analysis
1181 of an early methicillin-resistant Staphylococcus aureus strain and a biofilm-producing
1182 methicillin-resistant Staphylococcus epidermidis strain. J Bacteriol 187:2426-38.
1183 79. Horsburgh MJ, Aish JL, White IJ, Shaw L, Lithgow JK, Foster SJ. 2002. sigmaB
1184 modulates virulence determinant expression and stress resistance: characterization
1185 of a functional *rsbU* strain derived from Staphylococcus aureus 8325-4. J Bacteriol
1186 184:5457-67.
1187

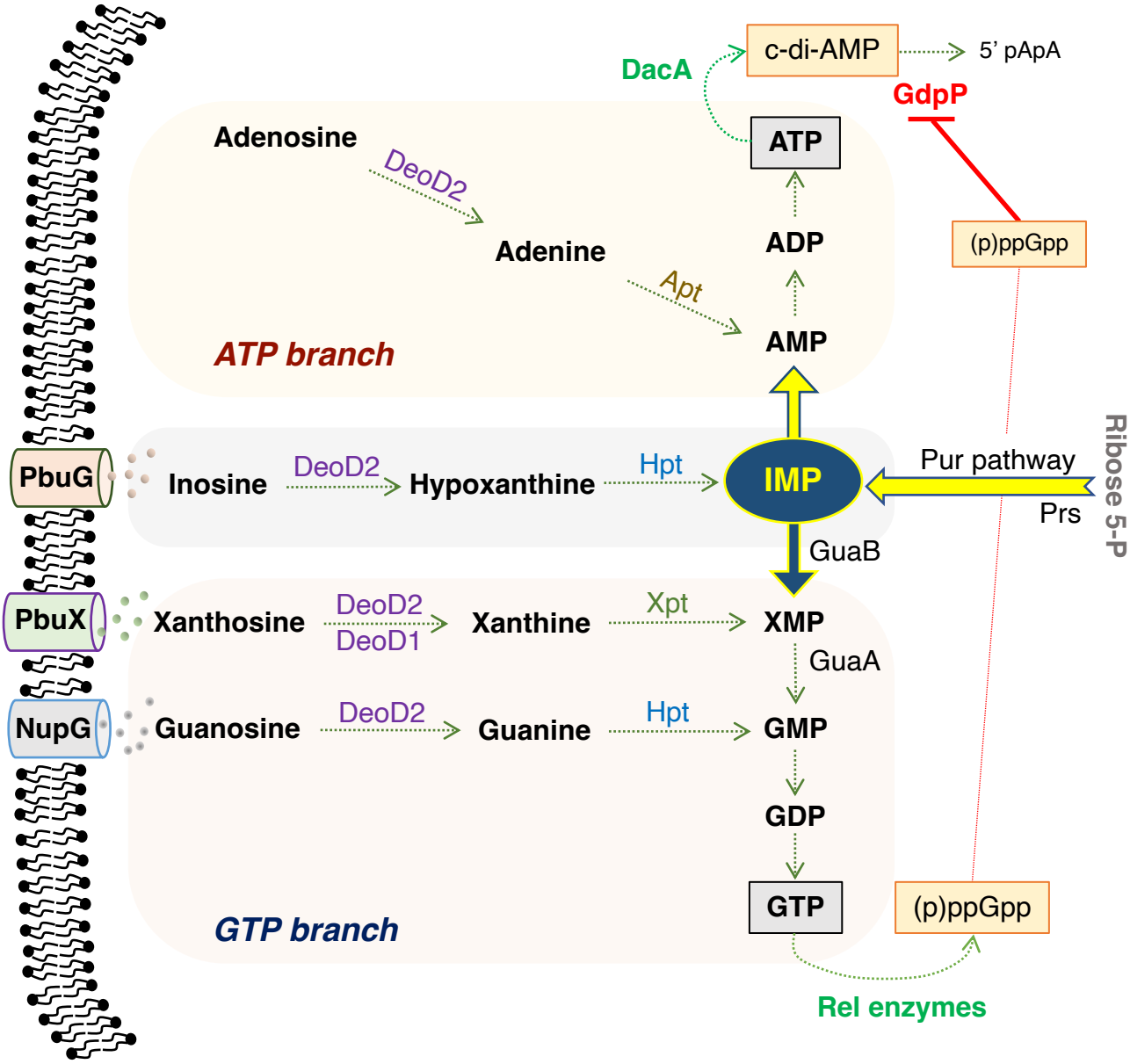
c-di-AMP
5' pApA
DacA
GdpP
Adenosine
DeoD2
ATP
Adenine
ADP
(p)ppGpp
Apt
AMP
ATP branch
PbuG
Inosine
DeoD2
Hypoxanthine
Hpt
IMP
Pur pathway
Prs
Ribose 5-P
GuaB
PbuX
Xanthosine
DeoD2
DeoD1
Xanthine
Xpt
XMP
GuaA
NupG
Guanosine
DeoD2
Guanine
Hpt
GMP
GDP
GTP
(p)ppGpp
GTP branch
Rel enzymes

Fig. 1.

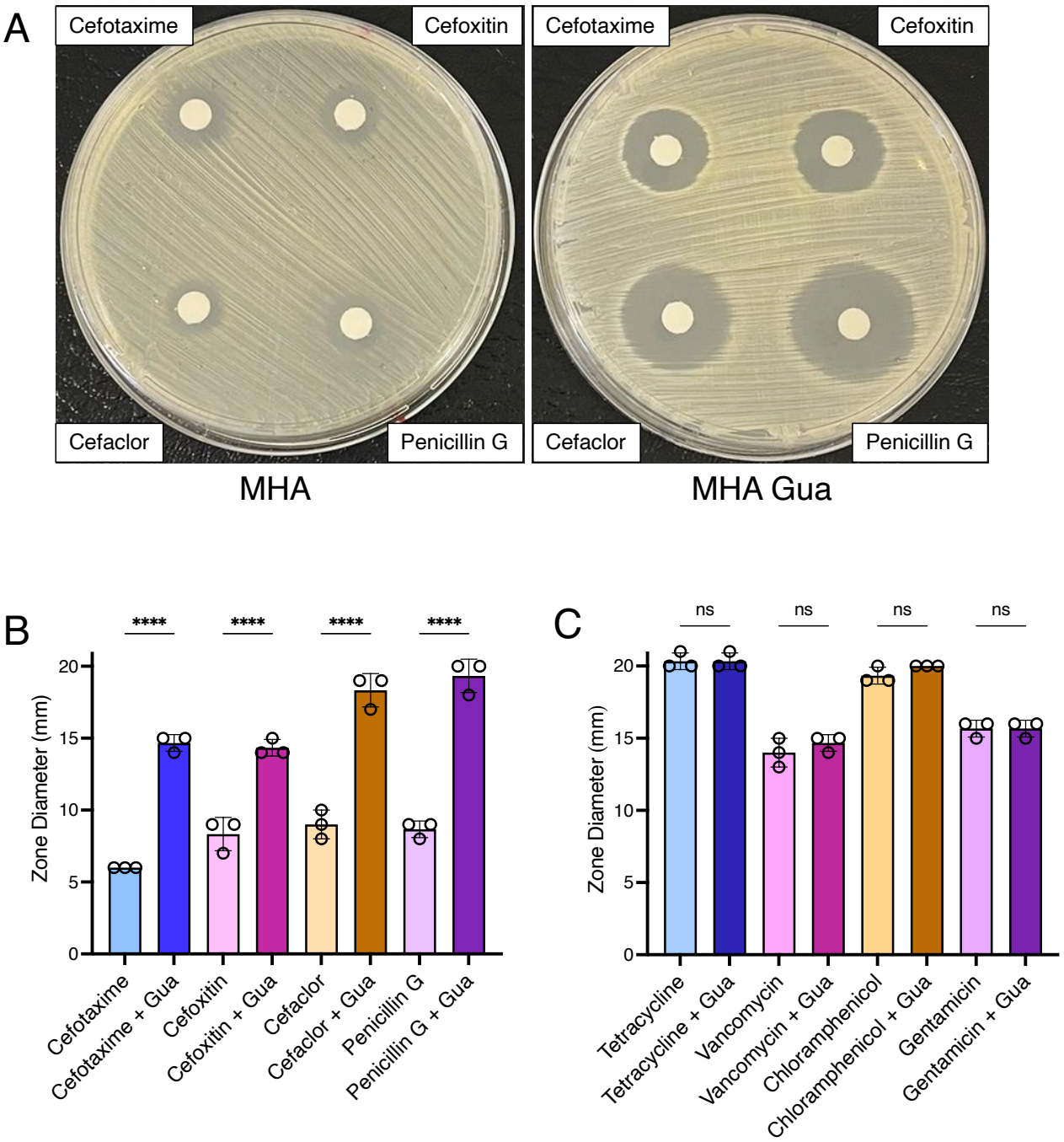
A
Cefotaxime
Cefoxitin
Cefaclor
Penicillin G
MHA
Cefotaxime
Cefoxitin
Cefaclor
Penicillin G
MHA Gua
B
****
****
****
****
Zone Diameter (mm)
0
5
10
15
20
Cefotaxime
Cefotaxime + Gua
Cefoxitin
Cefoxitin + Gua
Cefaclor
Cefaclor + Gua
Penicillin G
Penicillin G + Gua
C
ns
ns
ns
ns
Zone Diameter (mm)
0
5
10
15
20
Tetracycline
Tetracycline + Gua
Vancomycin
Vancomycin + Gua
Chloramphenicol
Chloramphenicol + Gua
Gentamicin
Gentamicin + Gua

Fig. 2.

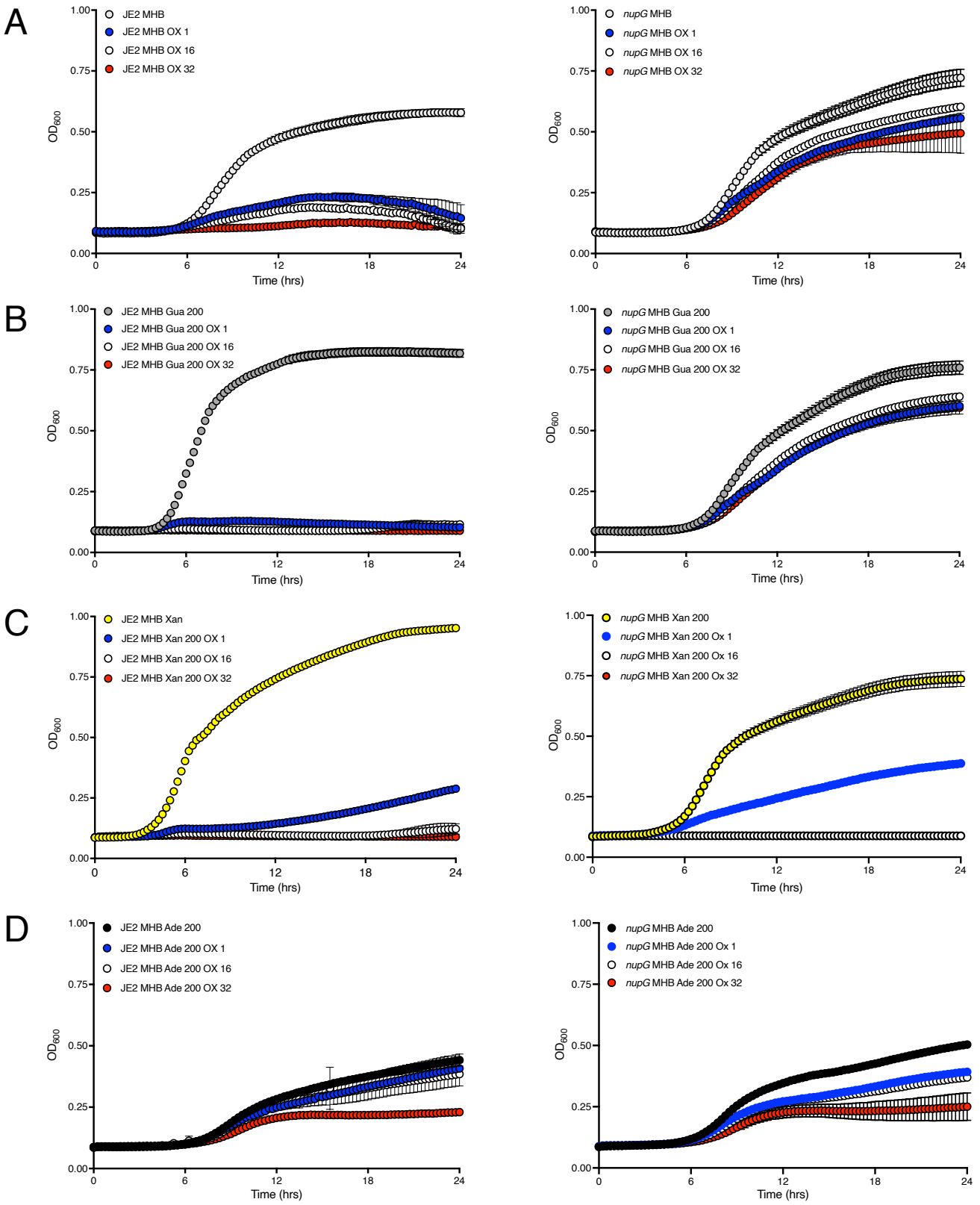
A
JE2 MHB
JE2 MHB OX 1
JE2 MHB OX 16
JE2 MHB OX 32
nupG MHB
nupG MHB OX 1
nupG MHB OX 16
nupG MHB OX 32
B
JE2 MHB Gua 200
JE2 MHB Gua 200 OX 1
JE2 MHB Gua 200 OX 16
JE2 MHB Gua 200 OX 32
nupG MHB Gua 200
nupG MHB Gua 200 OX 1
nupG MHB Gua 200 OX 16
nupG MHB Gua 200 OX 32
C
JE2 MHB Xan
JE2 MHB Xan 200 OX 1
JE2 MHB Xan 200 OX 16
JE2 MHB Xan 200 OX 32
nupG MHB Xan 200
nupG MHB Xan 200 Ox 1
nupG MHB Xan 200 Ox 16
nupG MHB Xan 200 Ox 32
D
JE2 MHB Ade 200
JE2 MHB Ade 200 OX 1
JE2 MHB Ade 200 OX 16
JE2 MHB Ade 200 OX 32
nupG MHB Ade 200
nupG MHB Ade 200 Ox 1
nupG MHB Ade 200 Ox 16
nupG MHB Ade 200 Ox 32
OD600
Time (hrs)
0.00
0.25
0.50
0.75
1.00
0
6
12
18
24

Fig. 3.

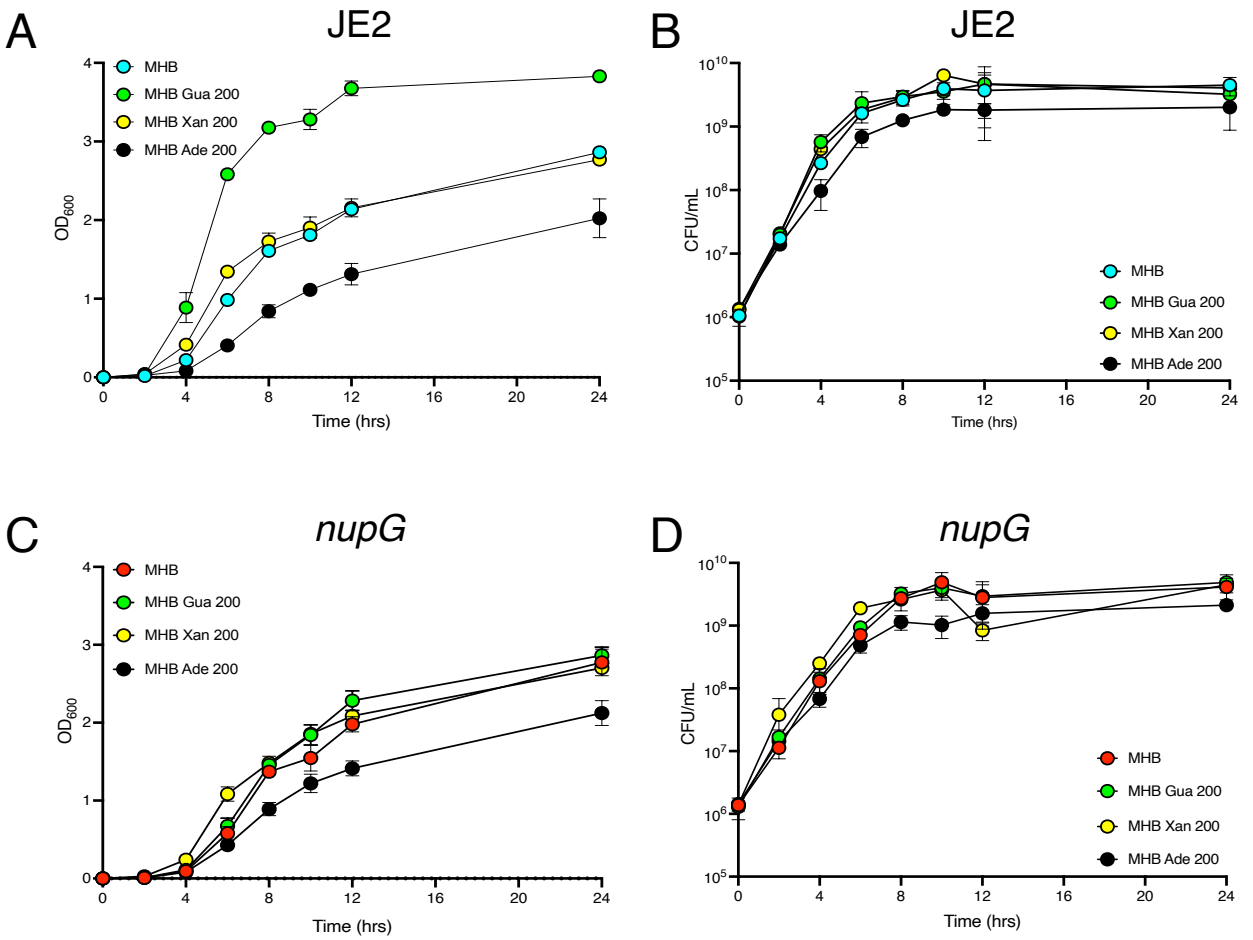
A
JE2
MHB
MHB Gua 200
MHB Xan 200
MHB Ade 200
OD600
Time (hrs)
B
JE2
CFU/mL
Time (hrs)
C
nupG
D
nupG

Fig. 4.

A

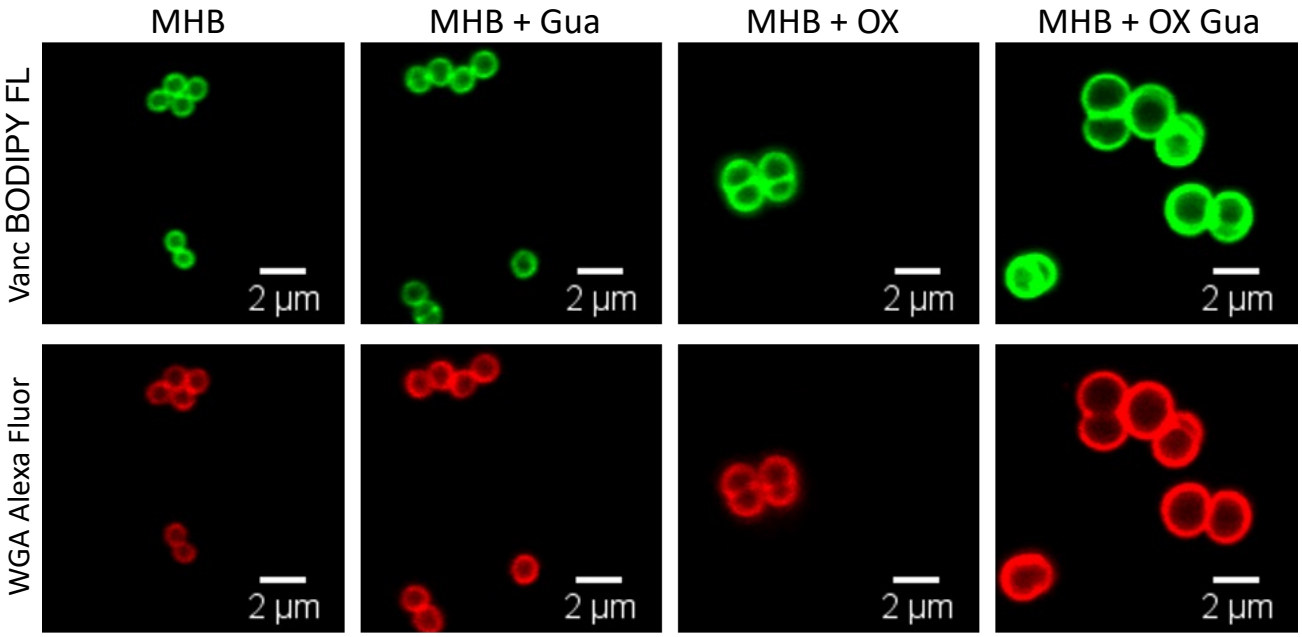
MHB
MHB + Gua
MHB + OX
MHB + OX Gua
Vanc BODIPY FL
WGA Alexa Fluor
2 µm

B

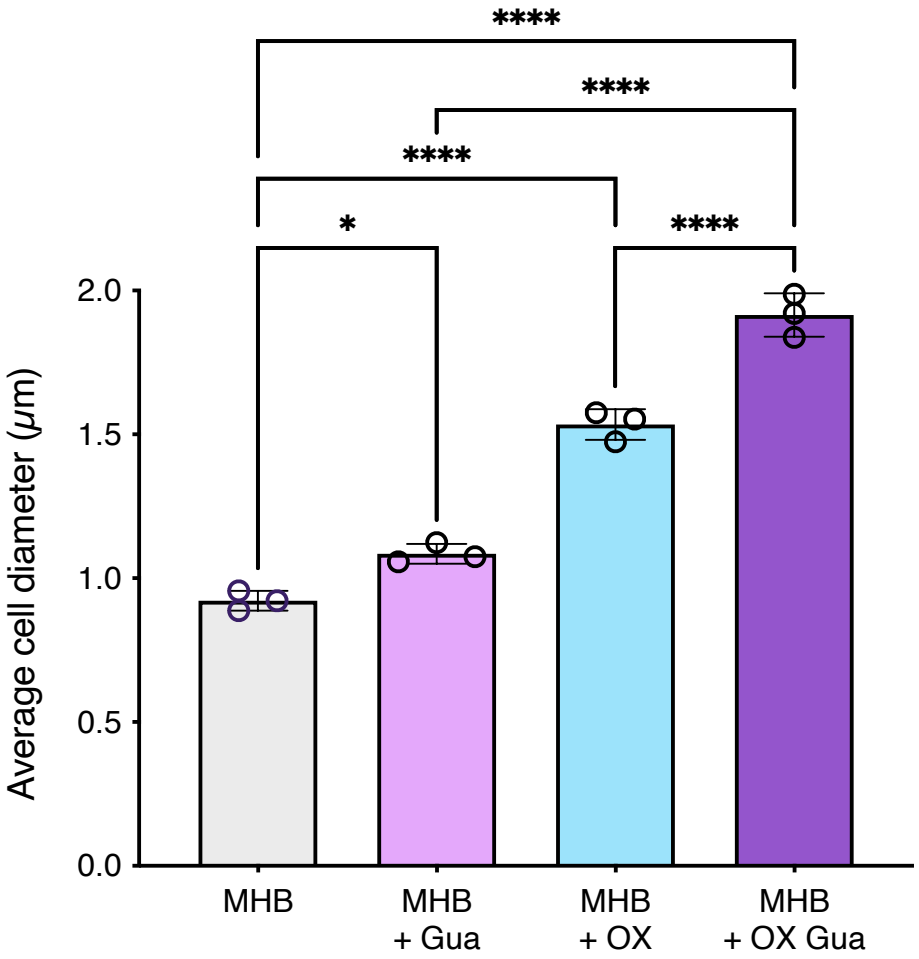
****
****
****
*
****
Average cell diameter (µm)
2.0
1.5
1.0
0.5
0.0
MHB
MHB + Gua
MHB + OX
MHB + OX Gua

Fig. 5.

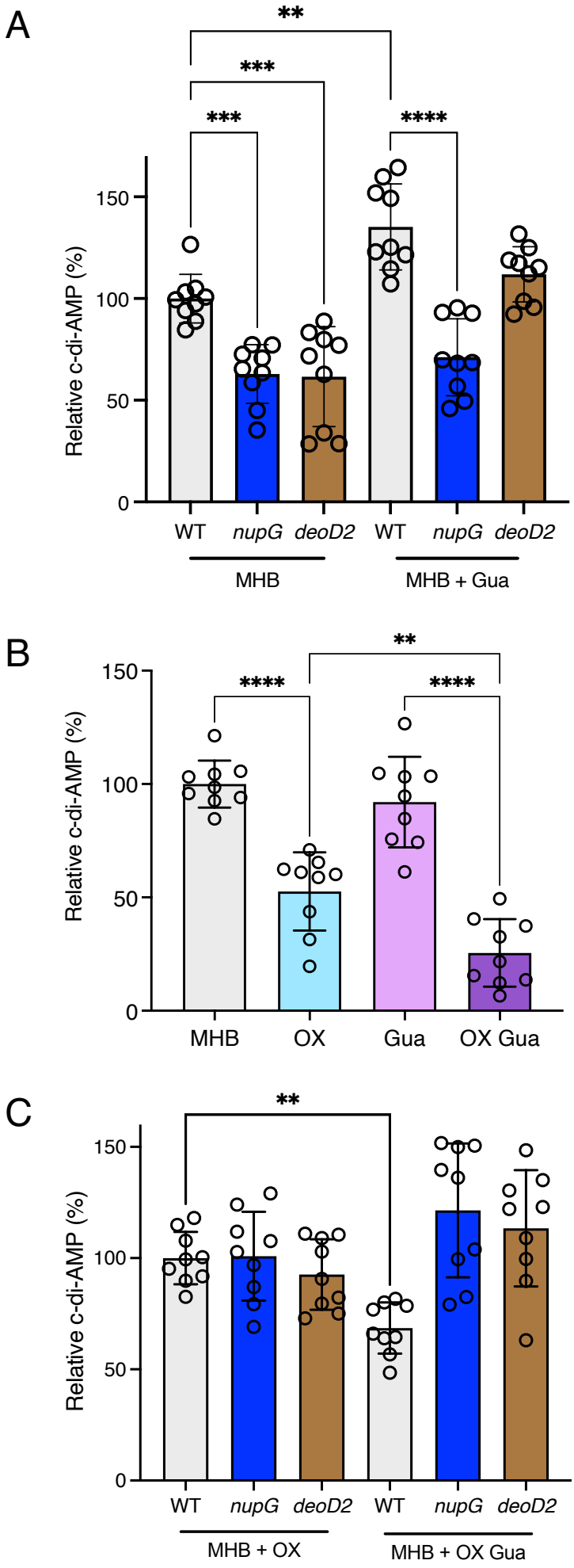
A
**
***
***
****
Relative c-di-AMP (%)
150
100
50
0
WT
nupG
deoD2
WT
nupG
deoD2
MHB
MHB + Gua
B
**
****
****
Relative c-di-AMP (%)
150
100
50
0
MHB
OX
Gua
OX Gua
C
**
Relative c-di-AMP (%)
150
100
50
0
WT
nupG
deoD2
WT
nupG
deoD2
MHB + OX
MHB + OX Gua

Fig. 6.